Pharmacological PARP-1 Inhibition Against Hypertensive Target Organ Damage in a Chronic Animal Model

Ph.D. Thesis

Author: Krisztián Erős, MSc.

Program Leader: Prof. Kálmán Tóth, M.D., DSc.

Project Leader: Róbert Halmosi, M.D., Ph.D.

1st Department of Medicine
University of Pécs, Medical School
Hungary

2017

Table of contents

Abbreviations 4

1. Introduction 6

1.1. Hypertension and related complications 6

1.2. The Spontaneously Hypertensive Rat as an animal model for chronic hypertension and target organ damages 6

1.3. Pathophysiological background of hypertension: role of ROS and inflammation 7

1.4. Processes in chronic hypertension-related cardiovascular remodeling and tissue damage 10

1.5. The Hippocampus as a model area of chronic hypertension-related target organ damage 12

1.6. Mitochondrial fusion/fission as a dynamic response to oxidative status in the heart: roles in mitochondrial adaptation and quality control 13

1.7. Physiological functions of the nuclear PARP-1 enzyme and its role during stress 14

2. Objectives / Specific Aims 18

3. Materials and Methods 20

3.1. Chemicals 20

3.2. Animals 20

3.3. Blood pressure measurement 21

3.4. Assessment of Intima-Media Thickness of carotid arteries, *in vivo* 21

3.5. Isometric force measurement of carotid arteries 21

3.6. Confocal laser scanning fluorescence microscopy 22

3.7. Histochemical observations 22

3.7.1. Carotid arteries 22

3.7.2. Dorsal hippocampus 23

3.8. Immunohistochemistry 23

3.8.1. Carotid arteries 23

3.8.2. Dorsal hippocampus 24

3.9. Transmission electron microscopy 24

3.10. Western blot 25

3.10.1. Whole cell preparations 25

3.10.2. Subcellular fractionation 25

3.10.3. Electrophoresis and transfer of proteins 25

3.11. Statistical analysis 26
4. Results 27
4.1. Specific Aim 1. Evaluation of chronic hypertension-induced vascular remodeling in SHR animals at the level of carotid arteries, in light of long-term pharmacological inhibition of PARP-1. 27
4.1.1. Long term L-2286 administration attenuated structural remodeling of carotid arteries in the SHR strain 27
4.1.2. Endothelial dysfunction in SHR animals was accompanied by elevated $ONOO^-$ formation 28
4.1.3. In carotid arteries of hypertensive rats, long-term L-2286 treatment mitigated AIF translocation and interfered with MAPK and NF-κB signaling 30
4.2. Specific aim 2. Observation of chronic hypertension related alterations of the dorsal hippocampus in the SHR strain, focusing on the level of oxidative stress and cell death events. 32
4.2.1. Structural alterations of the dorsal hippocampus in the hypertensive animals 32
4.2.2. Systemic L-2286 administration in SHR animals attenuated oxidative damage in the area of dorsal hippocampus 33
4.2.3. Long-term L-2286 administration attenuated pyramidal cell loss in the CA1 area of treated SHR animals 34
4.3. Specific aim 3. To elucidate evidences of mitochondrial protection achieved by long-term PARP-1 inhibition in the myocardium. 37
4.3.1. Ultrastructural observations on the interfibrillar mitochondria population in the myocardium 37
4.3.2. Quantifying the actual state of interfibrillar mitochondrial dynamics 38
4.3.3. Effects of L-2286 treatment on cellular levels and subcellular distributions of fusion-fission regulators. 39
5. Discussion 41
6. Novelty of findings 50
7. Publications of the author 51
7.1. Relevant publications 51
7.2. Additional publications 51
7.3. Published abstracts 53
8. References 56
9. Acknowledgement 62

Abbreviations

4-HNE	4-hydroxynonenal
8-OxG	8-oxoguanine
ACh	acetylcholine
AIF	apoptosis inducing factor
AKT-1	v-akt murine thymoma viral oncogene homolog 1
AMP	adenosine monophosphate
AMPK	AMP-activated protein kinase
Ang2	angiotensin 2
ANOVA	analysis of variance
ATF4	activating transcription factor-4
ATP	adenosine triphosphate
BBB	blood-brain barrier
BH4	tetrahydrobiopterin
CA	cornu ammonis region
CCA	common carotid artery
CRM1	chromosome region maintenance 1/exportin1
CSF	cerebrospinal fluid
DAB	3,3'-diaminobenzidine
DRP1	dynamin related protein-1
ECM	extracellular matrix
eNOS	endothelial nitric oxide synthase
ERK 1/2	extracellular signal–regulated kinase 1/2
ETC	electron transport chain, mitochondrial
GAPDH	glyceraldehyde 3-phosphate dehydrogenase
GD	gyrus dentatus
GFAP	glial fibrillary acidic protein
GTP	guanosine triphosphate
H_2O_2	hydrogen peroxide
IFM	interfibrillar mitochondria
IMT	intima-media thickness
iNOS	inducible nitric oxide synthase
IQ range	interquartile range
JNK1	c-jun n-terminal kinase 1

MAPK	mitogen-activated protein kinase
MKP-1/DUSP1	MAPK phosphatase-1
MMPs	matrix metalloproteinases
NAD^+	nicotine-adenine dinucleotide
NADPH	nicotine-adenine dinucleotide phosphate
NF-κB	nuclear factor kappa-light-chain-enhancer of activated B cells
NMNAT1	nicotinamide mononucleotide adenylyltransferase 1
NO	nitrogen monoxide
Noxs	nicotine-adenine dinucleotide phosphate oxidases
NT	nitrotyrosine
$O2^-$	superoxide anion
OH^-	hydroxyl radical
OMM	outer mitochondrial membrane
$ONOO^-$	peroxynitrite
OPA1	optic atrophy protein-1
p38 MAPK	p38 mitogen-activated protein kinase
PAR	poly-(ADP-ribose)-polymer
PARG	poly-(ADP-ribose)-glycohydrolase
PARP-1	poly(ADP)ribose-polymerase-1
PBS	phosphate buffered saline
PDC	pyruvate dehydrogenase complex
PFA	paraformaldehyde
RAAS	renin-angiotensin-aldosterone system
RIP1	receptor interacting serine/threonine kinase 1
ROS	reactive oxigene species
RT	room temperature
SBP	systolic blood pressure
SHR	spontaneously hypertensive rat
SNP	sodium nitroprusside
TBS	Tris-buffered saline
TBST	Tris-buffered saline
TRAF2	tumor necrosis factor receptor-associated factor 2
vSMC	vascular smooth muscle cell
WKY	wistar-kyoto rat

1. Introduction

1.1. Hypertension and related complications

Arterial hypertension represents a major cardiovascular epidemic condition, with a prevalence of more than 25% throughout the adult population, affecting nearly one billion individuals around the globe[1]. It remains asymptomatic until later in its course, but as a long-term consequence of this condition, accumulating damage in specific organs propagates the development of cardiac pathologies, renal failure, cerebrovascular pathologies and vascular dementia, atherosclerotic vascular disease and retinopathy[2]. Several processes are involved in these pathogenic alterations including endothelial activation, growth and migration of vascular smooth muscle cells, expression of pro-inflammatory mediators, changes in collagen turnover and the remodeling of extracellular matrix[3, 4]. Complex biochemical, hormonal and hemodynamic mechanisms form the basis of these alterations, referred as hypertensive target organ damage, however, the common ground is the excess generation of reactive oxygen species/ROS[2, 5], which, in addition to governing these pathological changes, possesses direct damaging properties[6]. Additional factors accompanying chronic hypertension may amplify these processes, including arterial stiffness, effects of sympathetic over-activity, dysregulation of tissue perfusion and increased activity of several hormone systems, especially the renin-angiotensin-aldosterone system/RAAS[2, 5].

1.2. The Spontaneously Hypertensive Rat as an animal model for chronic hypertension and target organ damages

The Spontaneously Hypertensive Rat/SHR strain was developed in the 1960's by Professor Kyuzo Aoki and colleagues, via the selective inbreeding of Wistar-Kyoto /WKY rats with consistently elevated blood pressure[7, 8]. Since then, it has become one

of the most intensively studied organisms in experimental cardiology with pathologies resembling human essential hypertension. The age-dependent development of high blood pressure has a polygenic background in the SHRs and based on renal transplant experiments, the kidneys play a particularly crucial role in this phenotype[9].

SHRs are normotensive at birth and develop stable blood pressure of 160-180 Hgmm at the age of 6-8 weeks. Following an additional increase in blood pressure, at 40-50 weeks, SHRs feature overt signs of cardiovascular pathologies related to chronic hypertension. Cardiac hypertrophy and fibrotic tissue accumulation have been described as a phenotypic trait of this strain with a concomitant transition towards heart failure through aging[10-12]. Additionally, the structural remodeling of various vessel segments and functional alterations as endothelial dysfunction and altered vascular permeability have been described in this strain[13, 14], conjoined with metabolic defects in lipid homoeostasis[15].

Numerous studies demonstrated the importance of an inflammatory status and oxidative stress in the cardiovascular system and other tissues of this strain, driving the pathological alterations consequent to the chronically elevated blood pressure[16, 17].

In the last decade, the SHR strain entered the scope of neurological research as an animal model of attention deficit hyperactivity disorder[18], and, also in the field of vascular dementias[19]. Regarding the latter pathology, SHRs can be distinguished from its stroke-prone counterpart, which is characterized by the focal tapering of arterial walls, which predisposes this strain to aneurysms and intracranial hemorrhage[20]. Rather, vascular alterations related disturbances in cerebral blood-flow regulation[21] and the presence of ischemic perivascular white matter damage[22] and cortical atrophic alterations make the SHR strain a feasible model for chronic neuronal diseases evolving on the grounds of elevated systemic blood pressure[19, 22-25].

1.3. Pathophysiological background of hypertension: roles of ROS and inflammation

Reactive oxygen species/ROS, such as superoxide anion/O_2^- and hydroxyl radical/OH^-, are chemical molecules containing oxygen with unpaired electrons in their outer orbit, resulting in high reactivity towards biomolecules. In the vasculature, these species are formed by all cellular components as endothelial cells, smooth muscle

fibers, fibroblasts and activated immune cells[2]. While various kinds of ROS physiologically participate in angiogenesis, vasomotor and permeability regulation, an imbalance in their production and elimination during pathological situations, defined as oxidative stress, leads to long-term phenotypical changes in the cardiovascular system[5, 6]. In addition to the direct tissue damaging properties of excess ROS production, it is also capable of modulating key intracellular signaling routes[6], mediating the phenotypic effect of the oxidative status on cellular components, and the reorganization of extracellular matrix[3]. In this way, the excess ROS production contributes substantially to the functional and structural remodeling of the cardiovascular system during acute stress scenarios and throughout chronic pathologies[3]. Accordingly, a pro-oxidant state with inflammatory markers in the vessels of human patients and animal models precedes the development of elevated blood pressure, demonstrating the fundamental role of the oxidative status in the local vascular milieu, and also in central regulators during the pathogenesis of hypertension[16, 26, 27]. Furthermore, the pivotal role of oxidative stress has been demonstrated in the initiation and development of vascular dysfunction and tissue damage associated with aging[28-30] and diseases, such as ischemic heart disease and acute coronary syndromes, stroke, hypertension[2], atherosclerosis[31] and diabetes mellitus[32]. Based upon these premises, modulating levels of tissue oxidative status or the cellular stress response elicited by it bears therapeutic potential and is protective against hypertension-induced target organ damage[2].

Amongst the enzyme complexes responsible for physiological ROS production, the nicotine-adenine dinucleotide phosphate oxidases/NOXs are one of the primary sources in the cardiovascular system[2]. These are membrane-bound enzymes, transferring electrons from NADPH to molecular oxygen to produce $NADP^+$ and O_2^-. In the vasculature, an increase in the activity and expression of various NOX enzymes, initiated by humoral and mechanical factors, has been demonstrated in a number of physiological and pathological conditions associated with vascular remodeling[2, 3]. In hypertension, angiotensin 2/Ang II appears to be the primary inducer, the activity of which is also associated with the vascular remodeling process by additional ROS-mediated signaling routes[2, 5, 6], including the activation of NOXes and Xanthine oxidases. Furthermore, in conjunction with immunological processes due to damage of the vascular endothelial layer, induction of various NOX enzymes via cytokine

signaling further boosts ROS production in the vasculature by the invading immune cells[3, 33, 34].

Superoxide anion may also originate from the mitochondrial electron transport chain/ETC as a by-product while transferring electrons from NADH to molecular oxygen. During episodes of tissue ischemia and cellular hypoxia, the mitochondrial ETC becomes uncoupled, leading to augmented O_2^- generation[21]. In pathologies accompanied by an elevated oxidative status, intracellular ROS originating primarily from activated NOX enzymes induce damage and inactivation of various ETC enzymes, leading to reduced mitochondrial transmembrane potential and mitochondrial dysfunction, characterized by a further boost in ROS production, which in excess amounts, overwhelm the capacity of intracellular antioxidant systems[2]. In this way, the mitochondria are both the source and the target of augmented ROS production[26], and its sensitivity is determined by the actual metabolic status of the cells and the capacity of compensatory mechanisms. In relationship to chronic hypertension, the uncoupling of the ETC due to the ischemic environment related to improper blood supply greatly contributes to the augmented ROS generation, leading to oxidative damage throughout the supplied tissues[2, 21]. During prolonged stress, accumulating damage worsens mitochondrial functionality and the stress signaling routes that mostly converge on the mitochondria eventually initiate cell death. In these mitochondria-dependent cellular demise processes, dissipation of the mitochondrial transmembrane potential and the permeability transition of the outer mitochondrial membrane/OMM for the release of ions and cell death effector proteins are early points of no return[35-37]. Therefore, therapeutic efforts are made to maintain mitochondrial functionality and stabilization of the OMM during acute and chronic stress scenarios.

Endothelial nitric oxide synthase/eNOS is one of the three isoforms of nitrogen monoxide/NO synthases which use L-arginine and molecular oxygen for the generation of NO, a potent vasodilator participating in blood pressure regulation. In the oxidatively stressed vasculature, the produced NO quickly reacts with O_2^- to form the highly reactive peroxynitrite/$ONOO^-$[38]. This reaction, in the process of reducing NO bioavailability, leads to the dysregulation of vascular tone[39], and its product also potentially induces damage of lipoproteins by forming nitrotyrosine/NT adducts, altering their structure and function[38, 40]. $ONOO^-$ is also a potent inducer of oxidative DNA modification, and in this manner, activates the nuclear enzyme poly(ADP)ribose-polymerase-1/PARP-1[38, 40, 41], a DNA damage sensor positioned centrally in the

cellular stress response. Under certain circumstances, when the levels of its co-factor tetrahydrobiopterin/BH4 or its substrate L-arginine are insufficient, eNOS transfers electrons from NADH directly to molecular oxygen, resulting in O_2^- generation, instead of NO production. This process, commonly referred to as eNOS uncoupling[3, 5], is the result of an insufficiency in the production or regeneration of BH4, or its degradation via oxidation by $ONOO^-$[42]. With aging and under pathological conditions, tissue arginases become highly expressed and reduce the bioavailability of L-arginine. Additionally, $ONOO^-$ is also capable of directly increasing arginase activity, propagating eNOS uncoupling and additional O_2^- generation[2].

During tissue inflammation, accompanying chronic hypertension, NO produced by the inducible form of NOS/iNOS, may form the basis of additional tissue $ONOO^-$ formation[27, 43]. The above mechanisms represent an intertwined network of processes which escalate vascular ROS formation in a feed-forward manner to the dysregulation of vascular tone inducing phenotypic changes and direct damage of the supplied tissues, delineating the role of ROS produced by various sources in the pathogenesis and consequences of chronic hypertension.

1.4. Processes in chronic hypertension-related cardiovascular remodeling and tissue damage

During chronic hypertension, as a resultant of hemodynamic factors, altered neurohumoral activity and an imbalance in vasodilator and constrictor forces, the vasculature display adaptive changes that influence their diameter and vasomotor responses governed by the structural reorganization of the vascular wall[44], which changes involve the cellular components and the extracellular matrix/ECM, constituting the remodeling process[3, 21]. It is accompanied by cytoskeletal reorganization, migration, growth and proliferation or death of cellular components and ECM alterations with changed collagen turnover[2, 45]. In addition to its direct damaging properties, ROS also functions as an important intra- and intercellular second messenger modulating many downstream signaling molecules, therefore, its augmented presence drives various aspects of these phenotypic changes[6] (Fig.1). Mechanically, it leads to hypertrophic or eutrophic remodeling of the vascular wall with or without changes in the lumen diameter dependent on the hemodynamic and

neurohumoral factors affecting the given vascular segment[44]. Various signaling routes mediate these effects in which Ang II initiated ROS-dependent signaling processes and activation of the mitogen-activated protein kinase/MAPK system possess dominant contribution[6, 46].

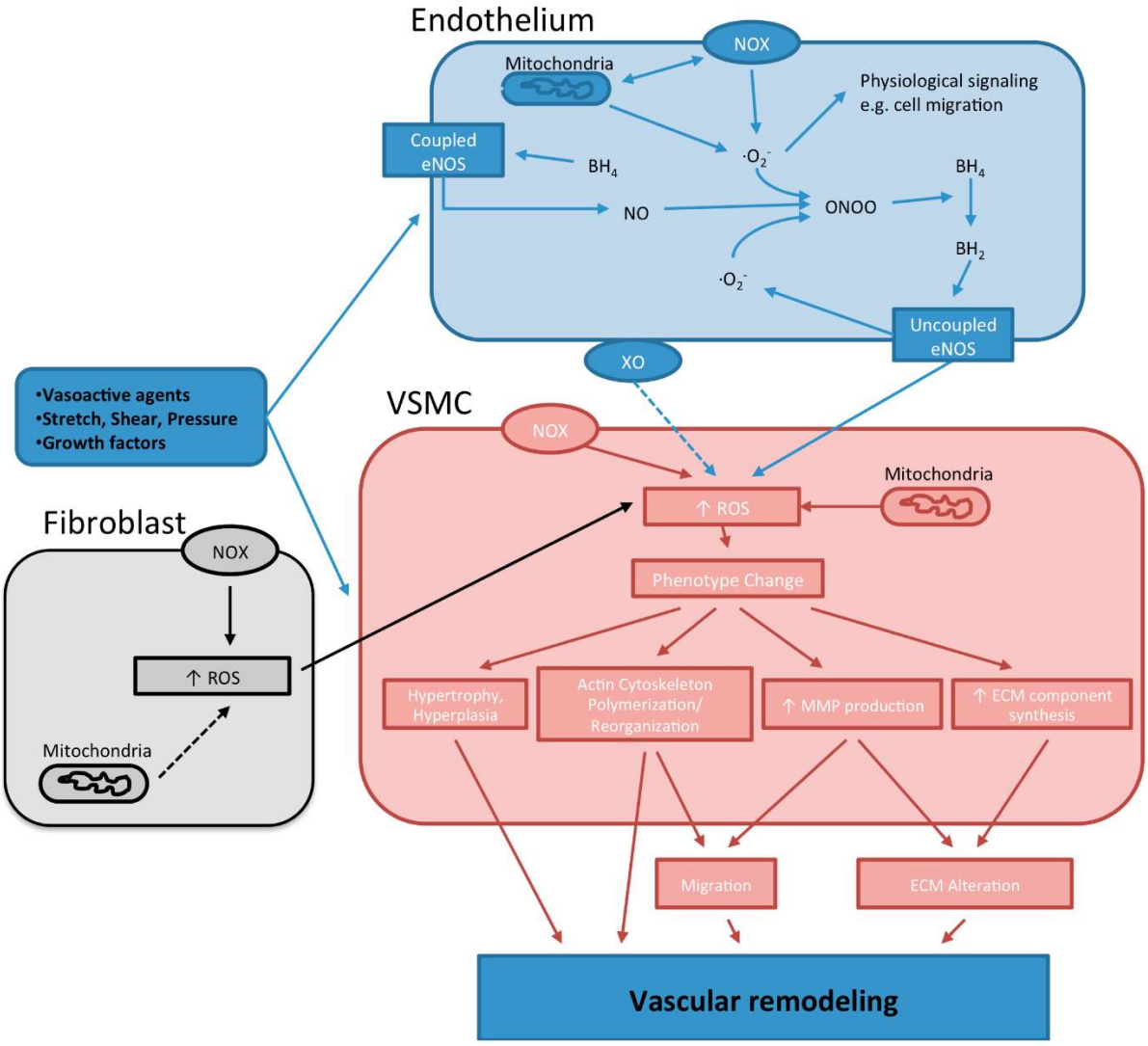

Figure 1. Reactive oxygen species-dependent mechanisms underlying vascular remodeling. Various stimuli activate ROS-generating enzymes in the endothelium or vascular smooth muscle cells/VSMC. In the endothelial layer, activation of NOX results in the production of O_2^-, which may also induce an increased release of ROS from the mitochondria. The O_2^- produced can activate physiological signaling routes and/or interact with NO to produce $ONOO^-$. The latter process is especially important in the oxidatively stressed vasculature, as produced $ONOO^-$ interacts with and reduce the bioavailability of BH4, leading to eNOS uncoupling with further O_2^- production and reduction of NO levels. In VSMCs exogenous or endogenous ROS induce phenotypic changes involved in vascular remodeling. Staiculescu et al. Int J Mol Sci; 2014 15(12):23792-23835

The initiated structural and functional alterations at the level of vasculature also lead to dysregulation of local tissue perfusion[3], resulting in improper oxygen and nutrient supply, and also in the accumulation of metabolic waste products. This way,

chronic hypertension-related vascular changes lead to compromised physiological functions of the supplied tissues, further contributing to the end-organ damage.

Alterations of the central nervous system on the grounds of chronic hypertension are primarily mediated by the cerebrovascular changes and deteriorated blood-brain barrier/BBB function induced by inflammatory processes and oxidative damage[21, 47, 48]. Excess ROS formation due to mitochondrial dysfunction carries deleterious effects in this highly energy-demanding organ by damaging lipoproteins, lipids and the DNA. Since the neuronal tissue is rich in unsaturated fatty acids, the oxidative damage of biomolecules leads to compromised neuronal functions and propagates cell death[2].

In regard to the heart, hypertension related alterations are primarily the results of the hypertrophic response of the cardiac wall, aiding to maintain cardiac work and oxygen supply of tissues in the face of altered peripheral resistance[49]. Above a specific threshold, the progression of wall thickening induces pathological changes due to the improper oxygen supply and metabolic alterations of the cardiomyocytes, resulting in structural remodeling accompanied by fibrotic tissue accumulation and cell death[49, 50]. These processes eventually lead to impaired heart function, and in this manner, propagates the development of cardiac dysfunction and a transition towards heart failure. Additionally, the deteriorated cardiac performance worsens proper perfusion of various tissues.

1.5. The Hippocampus as a model area of chronic hypertension-related target organ damage

The hippocampus is an allocortical portion of the temporal lobe. It is part of the core limbic system and plays important roles in consolidating short-term stored information into persistent memory engrams, and is crucial in the representation of the spatial position of the individual.

Hypertension represents a primary risk factor for chronic brain ischemia via the progressive remodeling of the cerebral vasculature, resulting in hypoperfusion[21, 23]. The hippocampus is particularly sensitive to ischemic insults and represents a predilection site for brain damage following disturbances in blood supply or dysfunction of the BBB[23, 25]. There are regional differences in its sensitivity regarding oxidative

insults, inducing neuronal damage especially in the area of cornu ammonis 1/CA1 subfield and the gyrus dentatus/GD, while pyramidal cells of the CA3 region are less affected[23] (Fig. 7). However, neurodegenerative processes of the hippocampus are studied mainly during acute ischemia/reperfusion damage, and in this regard, the SHR strain may represent a chronic animal model for hypertension-related cerebral pathologies. Circumscribed BBB dysfunction[22, 48, 51], hydrocephalus[52], atrophic alterations as the result of pyramidal cell loss[23], and reactive astrogliosis[23] as an indicator of a metabolically perturbative environment have been observed in the hippocampus of this strain[24]. These alterations are revealed in a relatively early stage of life and are connected to oxidative damage and inflammation accompanying chronic hypertension.

1.6. Mitochondrial fusion/fission as a dynamic response to oxidative status in the heart: roles in mitochondrial adaptation and quality control

Chronic hypertension bears an immense burden to the heart, inducing its hypertrophic response to accommodate the increased work demand. Initially an adaptive response, it may ultimately contribute to the progression of cardiomyopathies. Insufficient bioenergetic adaptation and disturbances in processes controlling mitochondrial quality have all emerged as key factors in the transition to pathological remodeling of the continuously working, highly energy-demanding cardiac muscle[53].

There are three subpopulations of cardiac mitochondria. The perinuclear and sub-sarcolemmal portion demonstrates high morphological heterogeneity, their functions are connected primarily to nuclear processes and membrane transport, respectively. The interfibrillar mitochondria/IFM subpopulation is densely packed between the contractile elements and have fundamental roles in ATP production and Ca^{++} buffering during the contractile process[54].

The view in which mitochondria are individual organelles in the cell has been challenged by the discovery of fusion and fission processes, which delineated a highly-interconnected network with dynamically regulated organization[36]. Main mediators of these processes have been identified in mammalian cells. The dynamin-related protein 1/DRP1 is a large GTPase constantly cycling between the cytosol and the OMM. To initiate fission, DRP1 is anchored permanently to the OMM by one of its receptors, then

polymerases into ring-like structures around the mitochondrion to separate it via constriction in a GTP-dependent manner[54, 55]. Various posttranslational modifications have been demonstrated to regulate mitochondrial translocation and GTPase activity of DRP1[36, 55]. Fusion of the OMM is mediated by Mitofusin 1 and 2, while the association of inner membranes requires the presence of Optic atrophy protein 1/OPA1, which also regulates the integrity of mitochondrial cristae membranes[54]. The cell constantly maintains an equilibrium of fusion-fission events, while a bias towards either process is an indicator of cellular adaptation to changing metabolic demand or various stressors[56, 57].

Originally there was a debate, whether processes of mitochondrial dynamics occur in the cardiac IFM subpopulation, given their dense organization and limited motility. However, as fusion and fission events participate in vital cellular functions, such as division and differentiation, and it is also required for proper mitochondrial homeostasis and quality control via selective mitophagy and mitochondrial biogenesis, a growing body of data indicates an imbalance in these processes has fundamental roles in the progression of cardiomyopathies[36, 54]. Accordingly, excess fragmentation of the mitochondrial reticulum has been demonstrated, accompanied by lowered transmembrane potential and augmented mitochondrial ROS production, in various models related to oxidative stress induced by hyperglycemic insult or ischemia/reperfusion damage[54]. Pharmacological or genetic interference of the fission process, or propagation of fusion activity, proved to be protective on mitochondrial function and apoptotic sensitivity in these acute stress scenarios[54]. Also, robust alterations in mitochondrial dynamics and reduced cellular levels of fusion regulators have been revealed during cardiac hypertrophy and, to a greater extent, in heart failure[54, 58, 59].

1.7. Physiological functions of the nuclear PARP-1 enzyme and its role during stress

PARP-1 is the most extensively studied representative of the PARP enzyme family including 17 putative members, based on the presence of PARP signature motif in their sequence. PARP-1 is an abundant nuclear protein with a modular structure, which by using NAD^+ as the substrate, catalyzes the covalent attachment of poly-(ADP-

ribose)/PAR polymers to acceptor proteins including histones, transcriptional complexes and the PARP-1 itself[35, 60, 61]. Given the negative charge of the polymer, this posttranslational modification alters the biochemical properties of the acceptor proteins regarding their structure, function, membership or localization[35]. The PAR polymer possesses a relatively short half-life, on a scale of minutes, as it is subsequently hydrolyzed by the enzymatic activity of PAR-glycohydrolase/PARG and ADP-ribosyl hydrolase 3. The polymer can also be detached from acceptor proteins and may function as signal transducers by binding to other proteins carrying PAR recognition modules or PAR-binding motifs[35, 61].

PARP-1 functions as a DNA damage sensor and participates in the recruitment and function of the DNA repair machinery under low or mild genotoxic damage. Also, via its interaction with various nuclear proteins like transcription factors and chromatin modifiers, it is capable of regulating wide-scale transcriptional programs in a chromatin-dependent manner[35]. During prolonged or excessive genotoxic stress, PARP-1 becomes hyperactivated and diminishes the nuclear NAD^+ pool. In this fashion, its excess activation limits the functionality of other NAD^+ dependent nuclear enzymes, such as the Sirtuins[60, 62, 63], and also drives the cell towards a metabolic catastrophe by impaired glycolysis and excess adenosine triphosphate/ATP usage. Originally, this mechanism was considered as the main initiator of the caspase-independent regulated necrosis, as stated by the Berger's suicide model[64]. In contrast, one of the first biochemical hallmarks of apoptosis is the proteolytic cleavage of PARP-1 by caspases, the purpose of which is presumably to prevent its activation by the fragmentation of DNA, and in this way, conserves cellular energy for the completion of the discrete removal of damaged cells[35]. The picture above was widened by the discovery, in which, during excessive PARP-1 activation, the accumulating PAR polymers translocate to the mitochondria, where it induces the release of the mitochondrial NADPH oxidase, apoptosis inducing factor/AIF and its translocation to the nucleus, leading to large-scale chromatin fragmentation. As a result, the PARP-1 initiated necroptosis subroutine is also referred to as parthanatos[35, 71], by the role of PAR-polymer formation and from the Greek personification of death, Thanatos (Fig.2). During PARP-1 mediated necroptosis, mitochondria may represent a key control point. In an oxidatively stressed cellular model, parthanatos was accompanied by gross mitochondrial depolarization, secondary O_2^- production and elevated intracellular Ca^{++} levels. Mitochondria also displayed the severely damaged ultrastructure of swollen

organelles, which alterations could be prevented by PARP-1 deficiency or its pharmacological inhibition[35, 65].

Traditionally, deleterious consequences of excess PARP-1 activation were studied in acute stress scenarios associated with oxidative DNA damage, such as ischemia-reperfusion or in models in which DNA damage was induced by alkylating agents or irradiation[61]. Later, profound roles of PARP-1 in tissue damage were also demonstrated in chronic diseases characterized by oxidative stress, such as diabetes mellitus or hypertension[61]. It functions in various pathogenic processes, as regulating inflammatory gene programs via nuclear factor kappa-light-chain-enhancer of activated B cells/NF-κB co-activation[66], or its interaction with MAPKs[67] (Fig.2).

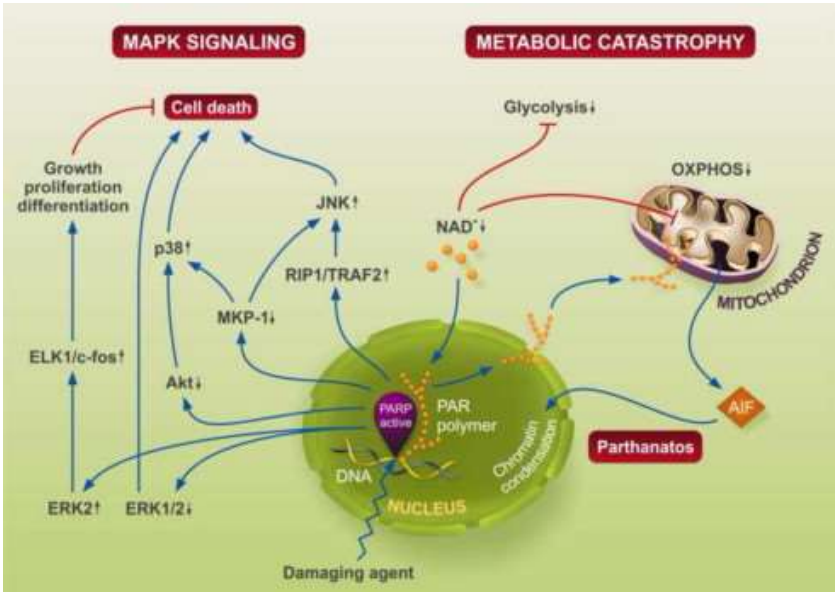

Figure 2. PARP-1 mediated cell death pathways. Activation of PARP-1 modulates various stress-responsive signaling pathways and its excess activation besides leading to cellular metabolic insufficiency also may initiate regulated necrosis via three major pathways that are likely to be tightly intertwined. Virág et al., Mol. Aspects Med. 2013 34(6):1153-67

Also, the observations in which activation and stability of PARP-1 are regulated by numerous stress-responsive signaling routes via posttranslational modifications, suggested its central role during the cellular stress response. By integrating various stress signals of intra- or extracellular origins and sensing the amount of DNA damage induced by these stressors, PARP-1 is capable of profoundly modulating well established cellular adaptation and stress response programs, taking part in cell fate decisions of growth and survival, or cellular demise[35]. Furthermore, due to its NAD^+ dependent enzymatic reaction, PARP-1 modify cell fate in a manner governed by the actual metabolic state of the cell. Recent results also suggested the sensitivity of PARP-1 to metabolic stressors. Its phosphorylation by AMP-activated protein kinase/AMPK has been shown to be required for the optimal activation of PARP-1 after

hydrogen peroxide/H_2O_2 exposure[68], also PARP-1 deficiency limited activation of AMPK during nutrient deprivation and delayed the autophagic response[69, 70] as a compensatory mechanism during starvation. As metabolic stress and hypoxia itself drive mitochondrial alterations and ROS production resulting in increased AMP/ATP ratio by DNA damage induced PARP-1 over-activation, these feed-forward mechanisms delineate an intertwined network of cellular stress signaling defining cellular fate, converging on PARP-1 activity.

2. Objectives / Specific Aims

We aimed to observe signs of the elevated oxidative stress in various tissues of SHR animals and elucidate mechanisms of their contribution to chronic hypertension-induced target organ damage, with a special emphasis on the role of PARP-1 activation during these processes.

Specific Aim 1. Evaluation of chronic hypertension-induced vascular remodeling in SHR animals at the level of carotid arteries, in light of long-term pharmacological inhibition of PARP-1.

Structural and functional remodeling of various vascular segments already described in the SHR animals includes damages and dysfunction of the endothelial layer, changes in lumen diameter and wall thickness with fibrotic tissue accumulation[14]. In this specific aim, at the level of carotid arteries, we monitor these processes strongly related to an elevated level of oxidative stress present in the vasculature of this strain. In addition to initiating oxidative DNA damage related cell death events, intracellular signaling interactions of PARP-1 activity in the stressed vasculature propagate its phenotypical changes. In this way, level and subcellular distribution of the main regulators of inflammatory processes and MAPK activity are assessed.

Specific Aim 2. Observation of chronic hypertension related alterations of the dorsal hippocampus in the SHR strain, focusing on the level of oxidative stress and cell death events.

One of the most deleterious consequences of hypertension-induced vascular remodeling is the inadequate perfusion of the supplied tissues. As the brain is a highly energy-demanding organ with low ischemic tolerance, attenuating the vascular alterations during chronic hypertension is presumably beneficial in various forms of dementias[22, 24]. Furthermore, the protection of neuronal tissue is highly dependent on the structure of BBB, the integrity of which is deteriorated in chronic hypertension due to inflammatory processes and endothelial damage[21, 48]. In this aim, in conjunction with pharmacological PARP-1 activity modulation, we specifically focus on markers of

oxidative stress related tissue damage and cell loss in the dorsal hippocampus, as a cerebral model area for target organ damage in the SHR strain.

Specific Aim 3. To elucidate evidence of mitochondrial protection achieved by PARP-1 inhibition in the myocardium.

During persistent hypertension, cardiac muscle adapts to the increased workload by hypertrophy. The metabolic adaptation capabilities of cardiac mitochondria are fundamental to maintain proper cardiac function during this compensatory phase. The mitochondria are highly dynamic organelles, which reacts to a perturbative environment by a shift in the fusion-fission equilibrium. Disturbed processes of mitochondrial quality control, biogenesis and a metabolic insufficiency propagate the progression cardiac dysfunction with myocyte loss, leading to eventual heart failure[58]. In this specific aim, we seek to make qualitative assessments on the ultrastructural level and to quantify the actual state of mitochondrial fusion-fission processes in the hypertrophied myocardium. Also, the effect of long-term L-2286 treatment on levels of DRP1 and OPA1 is assessed in whole cell preparation and subcellular fractions.

3. Materials and Methods

3.1. Chemicals

The water soluble PARP-1 inhibitor 2-[(2-Piperidine-1-ylethyl)thio]quinazolin-4(3H)-one (L-2286) (Fig.3) was a kind and generous gift of Professor Kalman Hideg and Professor Tamas Kalai, from the Department of Organic and Pharmacological Chemistry (Medical School, University of Pecs, Hungary). The compound was chosen from a group of experimental 4-quinazolinone derivatives, synthesized based on the crystal structure of the PARP-1 catalytic domain. *In vitro* measurements demonstrated an IC_{50} of 2.6 μM against isolated human PARP-1[71].

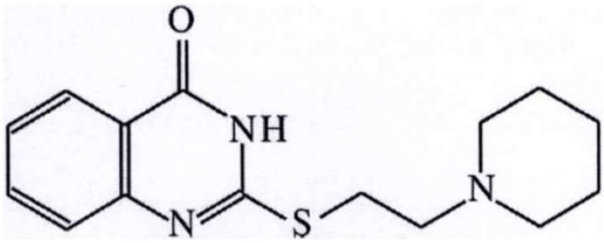

Fig 3. Chemical structure of L-2286 (2-[(2-Piperidine-1-ylethyl) thio] quinazolin-4 (3H)-one)

3.2. Animals

Male SHR animals aged at 10 weeks and serving in the role of normotensive controls, age-matched WKY rats were purchased from Charles River Laboratories (Budapest, Hungary). Animals were caged individually and maintained on a 12 h light/dark cycle at 24 °C. Following ultrasound examinations to exclude animals with carotid artery abnormalities, each strain was randomized into groups (n=15/group) receiving 5 mg/kg/day L-2286 treatment[11, 14, 72-74] (WKY-L and SHR-L) or not (WKY-C and SHR-C) for 32 weeks. L-2286 was dissolved in drinking water which was delivered in excess volumes in tightly capped vessels. The dosage was recalculated every two weeks based on data in reference to the mean volume of daily consumptions and weekly body weight measurements. No animal loss occurred during the treatment period. Animals were sacrificed following ketamine/xylazine anesthesia. The investigation conforms to the Guide for the Care and Use of Laboratory Animals published by the US National Institutes of Health and was approved by the Animal

Research Review Committee of the University of Pecs, Medical School (BA02/2000-2/2010).

3.3. Blood pressure measurement

Non-invasive blood pressure measurements were carried out every four weeks from the beginning of the study using the tail-cuff method (Hatteras SC 1000 Single Channel System)[75]. A heating pad was applied to prevent constriction of tail vessels. Three consecutive measurements of systolic blood pressure/SBP were averaged for each animal at every sequential points of time.

3.4. Assessment of Intima-Media Thickness of carotid arteries, *in vivo*

Two-dimensional ultrasound was performed under inhalation anesthesia at the beginning of the study and on the week of sacrifice. Rats were lightly anesthetized using a mixture of 1.5% isoflurane and 98.5% oxygen. The necks and the upper side of the chest of animals were shaved, acoustic coupling gel was applied, and a warming pad was used to maintain normothermia. Intima-media thickness/IMT of carotid arteries was measured using a VEVO 770 high-resolution ultrasound imaging system (Visual Sonics, Toronto, Canada) equipped with a 40 MHz transducer.

3.5. Isometric force measurement of carotid arteries

The method was performed in accordance with a standard protocol using common carotid arterial/CCA rings isolated from 4 rats each group. The isometric contractile force was measured by using standard bath procedures. Briefly, following ketamine/xylazine anesthesia, the carotid arteries were removed, quickly transferred to ice-cold oxygenated (95% O_2 and 5% CO_2) physiological Krebs solution and dissected into 5 mm rings. Each ring was positioned between two stainless steel wires in a 5 ml organ bath of a Small Vessel Myograph (DMT 610M, Danish Myo Technology, Aarhus, Denmark). A normalization procedure was performed to obtain the basal tone to 1.0 g (13.34 mN), and artery segments were allowed to stabilize for 60 minutes prior taking measurements. The software Myodaq 2.01 M610+ was used for data acquisition and display. The rings were pre-contracted and equilibrated for 60 minutes until a

stable resting tension was acquired. The bath solution was continuously oxygenated with a gas mixture of 95% O_2 plus 5% CO_2 and kept at 36.8°C (pH 7.4). Vasorelaxation is expressed as a percentage reduction of the steady-state tension, obtained with isotonic external 60 mM KCl. Cumulative response curves of carotid rings were obtained in the presence of increasing doses of sodium nitroprusside/SNP (10^{-9} to 10^{-5} M), or acetylcholine/ACh (10^{-9} to 10^{-5} M). Arterial rings showing relaxation to ACh of more than 30% were considered as endothelium-intact. At the end of the experiments, administration of 60 mM KCl was repeated towards effectively examining the viability of the carotid arteries. Each measurement was carried out on rings prepared from different rats.

3.6. Confocal laser scanning fluorescence microscopy

Left carotid arteries of four rats from each group were fixed immediately following excision in a buffered paraformaldehyde solution/PFA (4%) overnight at 4°C. Five micrometer thick sections were cut and processed for immunolabeling with antibodies recognizing AIF (Cell Signaling Technology #4642, 1:100), NF-κB (Cell Signaling Technology #13586, 1:200) and MAPK phosphatase-1/MKP-1 (Santa Cruz Biotechnology sc-370, 1:100). As the fluorochrome-labelled secondary antibody, donkey-anti-rabbit Northern Lights antibody (R&D Systems NL004, 1:200) was used. Sections were counterstained with Hoechst (Sigma) and examined using a confocal laser scan microscope (Olympus Fluoview 1000). Recording for Rhodamine Red™-X (excited with 557 nm Helium-Neon laser) was followed by recording for Hoechst with a 405 nm laser.

3.7. Histochemical observations

3.7.1. Carotid arteries

Paraffin-embedded carotid slices were stained with Masson's trichrome to detect interstitial fibrosis and quantified with the NIH ImageJ analyzer system using the color deconvolution plugin to separate the blue collagen staining and measure its coverage[76]. Measurements were normalized to the tissue-covered area and presented

as area percentage (area%). Values of three non-overlapping segments of the tunica media on each preparation were averaged.

3.7.2. Dorsal hippocampus

Following ketamine/xylazine anesthesia and then thoracotomy, the aortic root was cannulated and the right femoral artery incised to ensure proper effluence. Animals were perfused with physiological saline solution to rinse blood away from the vasculature followed by buffered PFA. Following decapitation, the brain was removed, the hemispheres separated and post-fixed in PFA overnight at 4^{o}C. After embedding in paraffin, coronal sections were taken at the position of bregma approx. (-4.3) – (-3.8) (Paxinos&Watson). Slices were processed for Periodic acid-Schiff/PAS or Cresyl violet staining. Hippocampal pyramidal cell counting was limited between the CA1-CA2 border and the lowest point of CA1-enthorhinal cortex transition on Cresyl violet preparations. TUNEL test (R&D Systems, 4810-30-K) was conducted on embedded brain tissue samples in accordance with the manufacturer's protocol. Cell counting was conducted by multiple observers. All histological samples were acquired and examined by an investigator in blind fashion.

3.8. Immunohistochemistry

3.8.1. Carotid arteries

Carotid slices were also processed for NT (Millipore #06-284, 1:100) immunohistochemistry. Binding was visualized with biotinylated-horseradish peroxidase conjugated secondary antibody followed by the avidin-biotin-peroxidase detection system (PK-6200 Universal Vectastain ABC Elite Kit, Vector Laboratories, Burlingame, CA) using 3.3'-diaminobenzidine/DAB as chromogen. The progress of the immunoreaction was monitored under a light microscope and the reaction was paused by the removal of excess DAB with a gentle buffer wash.

3.8.2. Dorsal hippocampus

Brain sections were processed for immunohistochemistry with antibodies recognizing the following antigens: NT (Millipore #06-284, 1:100), 4-hydroxynonenal/4-HNE (a generous gift from Immunology and Biotechnology Department, Pecs, Hungary, 1:200), anti-PAR (Abcam ab14459, 1:400), 8-oxoguanine/8-OxG (Abcam ab64548, 1:500) and glial fibrillary acidic protein/GFAP (1st Degree Bio #Z0334, 1:500). Immunolabeling was visualized by DAB as a chromogen with Universal Vectastain ABC Elite Kit (Vector Laboratories, Burlingame, CA).

3.9. Transmission electron microscopy

Following ketamine/xylazine anesthesia and then thoracotomy, hearts were perfused in retrograde, through the aortic root with ice-cold phosphate buffered saline/PBS to rinse blood away, followed by modified Kranovsky fixative (2% PFA, 2, 5 % glutaraldehyde, 0, 1 M Na-cacodylate buffer, pH 7.4 supplemented with 3 mM $CaCl_2$). Next, 1mm thick sections were taken from the free wall of the left ventricle. After washing in phosphate buffer, the samples were incubated in 1% osmium tetroxide in 0.1 M PBS for 35 minutes. Subsequently, the samples were washed in buffer several cycles and dehydrated in an ascending ethanol series, including a step of uranyl acetate (1%) solution in 70% ethanol to increase contrast. Dehydrated blocks were submerged in Durcupan resin (Sigma) and then embedded in gelatine capsules containing Durcupan. 1 μm thick semithin and serial ultrathin sections (70 nm) were cut with a Leica ultramicrotome, and mounted either on mesh, or on Collodion-coated (Parlodion, Electron Microscopy Sciences, Fort Washington, PA) single-slot, copper grids. Additional contrast was provided to these sections with uranyl acetate and lead citrate solutions. The preparations were examined utilizing a JEOL1200EX-II electron microscope. Areas of IFM were measured by freehand polygon selection (n~500/group) in ImageJ software, where length of longitudinal axes and numbers of mitochondrial cristae were also evaluated.

3.10. Western blot

3.10.1. Whole cell preparations

50 mg of heart samples were homogenized in ice-cold isolation solution (50 mM Tris-buffer pH 7.4, 150 mM NaCl, 1 mM EDTA, protease inhibitor 1:100, phosphatase inhibitor 1:100 and sodium vanadate 1:100), and then samples were centrifuged at 750 G for 12 minutes. Supernatants were harvested in 2× SDS–polyacrylamide gel electrophoresis sample buffer and denaturated at 95°C for 5 minutess.

3.10.2. Subcellular fractionation

Heart tissue was minced in ice-cold isolation solution (150mM NaCl, 50 mM TRIS, 1mM EDTA, protease inhibitor 1:100, phosphatase inhibitor 1:100), and samples were disrupted on ice by Turrax, then processed in a Potter-Elvehjem tissue homogenizer. Centrifugation was carried out for 12 minutes at 750 g. Subsequently, supernatants containing the cytosolic and mitochondrial fractions were aspirated and the precipitate nuclear fraction was discarded. Next, supernatants were centrifuged for 12 minutes at 11,000 g to gain cytosolic fraction in the supernatant and mitochondrial in the precipitate. Samples were harvested separately in 2× SDS–polyacrylamide gel electrophoresis sample buffer and denaturated at 95°C for 5 minutes.

3.10.3. Electrophoresis and transfer of proteins

Proteins were separated on 7 or 10% SDS–polyacrylamide gels then transferred to a nitrocellulose membrane. After blocking (2 hours with 2% BSA in Tris-buffered saline/TBS), membranes were probed overnight at 4 °C with antibodies recognizing the following antigens: DRP1 (Cell Signaling Technology #8570, 1:1000), OPA1 (Santa Cruz biotechnology sc-393296, 1:500), anti-PAR (Abcam ab14459, 1:1000). As a loading control, Glyceraldehyde 3-phosphate dehydrogenase/GAPDH (Sigma Aldrich G8795, 1:4000) and pyruvate dehydrogenase complex (PDC, Thermo Fisher Scientific PA5-17190, 1:1000) were used for whole cell or cytoplasmic fraction and mitochondrial fraction, respectively. Membranes were washed six times for 5 minutes in TBS (pH

7.5) containing 0.1% Tween/TBST and three times for 5 minutes in TBS, preceding the addition of goat anti-rabbit/mouse horseradish peroxidase-conjugated secondary antibody (1:30000 dilution, Bio-Rad, Budapest, Hungary) and incubated at RT for 4 hours. The antibody–antigen complexes were visualized by means of enhanced chemiluminescence. Results were quantified in the NIH ImageJ program. Densities of bands were normalized to the respective loading controls.

3.11. Statistical analysis

Normal distribution of group data was checked by the Shapiro-Wilk test. Baseline comparisons between the strains were made by independent samples t-test. Measurements on carotid arteries and the dorsal hippocampus were analyzed by a strain x treatment two-way analysis of variance/ANOVA with 2 levels of each factor, followed by an independent samples t-test in case of factor interactions. On mitochondrial data, one-way ANOVA with Welch correction was conducted followed by Dunnet's *post hoc* test, to reveal the statistical significance of the differences compared to the SHR-C group. Due to the non-normal distribution of data, mitochondrial area and longitudinal axis length measurements were analyzed by the Kruskal-Wallis test followed by *post hoc* pairwise comparisons in SPSS 21.0. All data are presented as mean±S.E.M and $p<0.05$ was considered statistically significant.

4. Results

4.1. Specific Aim 1. Evaluation of chronic hypertension-induced vascular remodeling in SHR animals at the level of carotid arteries, in light of long-term pharmacological inhibition of PARP-1.

4.1.1. Long term L-2286 administration attenuated structural remodeling of carotid arteries in the SHR strain

Elevation of systolic blood pressure in the SHR strain was significant at the beginning of the study (WKY vs. SHR strain, $p<0.05$) (Fig. 4A). This difference was present throughout the treatment period (at the age of 42 weeks, strain factor: $p<0.01$). Long-term L-2286 treatment apparently did not exert any significant effect on SBP values compared to control groups at any time point.

Chronic hypertension induced arterial remodeling is characterized by thickening of the vascular wall via expansion of smooth muscle cells and an increased interstitial fibrosis[14, 44]. Therefore, we evaluated the IMT of carotid arteries. At baseline, the difference was not significant between the strains (Fig. 4B). At the age of 42 weeks, measurements of IMT in carotid arteries demonstrated profound alterations in control hypertensive animals, by nearly a two-fold increase in wall thickness (strain factor: $p<0.01$). Although PARP inhibition attenuated this elevated blood pressure induced process (SHR-L vs SHR-C, $p<0.05$), it did not have any significant effect in normotensive animals regarding this parameter. Quantifying area coverage of collagen bundles on Masson's trichrome stained sections, revealed an extensive accumulation in the middle portion of carotid walls of SHR-C animals at the age of 42 weeks (strain factor: $p<0.01$) (Fig. 4C,D). The lowered thickening of carotid walls in treated hypertensive rats was accompanied by a substantial decrease in collagen content compared to the control group (SHR-L vs. SHR-C, $p<0.01$). Comprehensively speaking, 32 weeks of L-2286 administration profoundly attenuated structural remodeling of carotid arteries regarding wall thickening (Fig. 4B) and fibrotic tissue accumulation (Fig. 4C,D). This effect may be partially independent of the elevated

blood pressure, as applied treatment did not modify this parameter in either strain in a statistically significant manner (Fig. 4A).

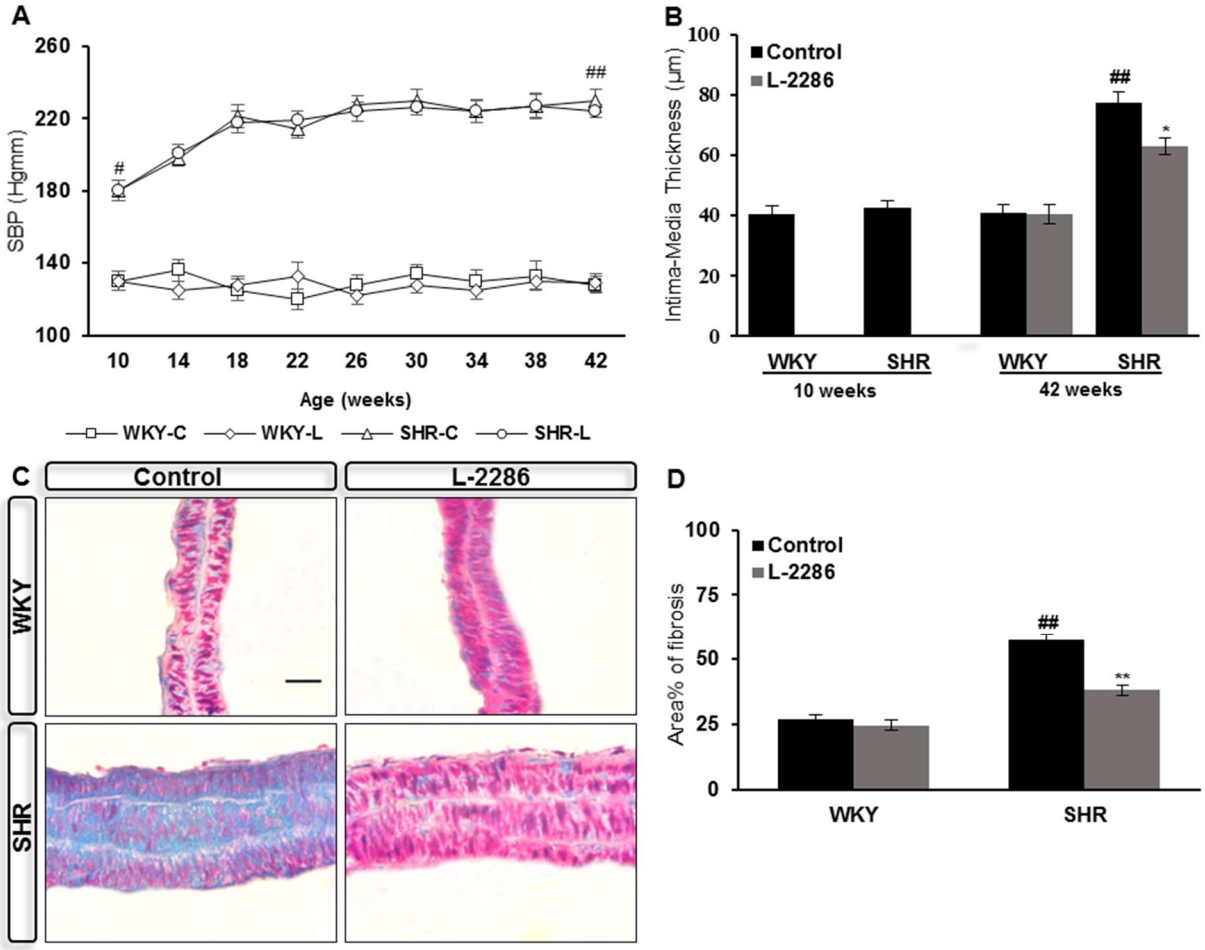

Figure 4.: Long-term L-2286 administration attenuated structural remodeling of carotid arteries without affecting blood pressure in SHR animals. (A) SBP of animals, measured every 4 weeks during the treatment period. (B) IMT of carotid arteries measured by ultrasound imaging at the beginning and at the end of the study. (C) Representative Masson's trichrome stained micrographs (scale bar 30 µm) and (D) quantification of collagen content of carotid artery walls. Data are presented as mean±S.E.M. $^{\#}p<0.05$, $^{\#\#}p<0.01$ vs. WKY-C; *p<0.05, **p<0.01 vs. respective controls.

4.1.2. Endothelial dysfunction in SHR animals was accompanied by elevated $ONOO^-$ formation

During the pathogenesis of hypertension, a boosted production of O_2^- in the vasculature leads to vasomotor disturbances by reacting with the potent vasodilator NO, to form $ONOO^-$ [3]. As the latter product is highly reactive, it has direct damaging properties against nucleic acid and lipoproteins, and, in this way, results in additional tissue damage and vascular dysfunction related to the elevated oxidative status. Visualizing $ONOO^-$ modified lipoprotein content of carotid walls by

immunohistochemistry revealed an extensive accumulation of nitrated tyrosine residues in SHR-C animals compared to normotensive rats (Fig. 5A). Long-term L-2286 treatment attenuated level of oxidative stress and NT formation in both strains.

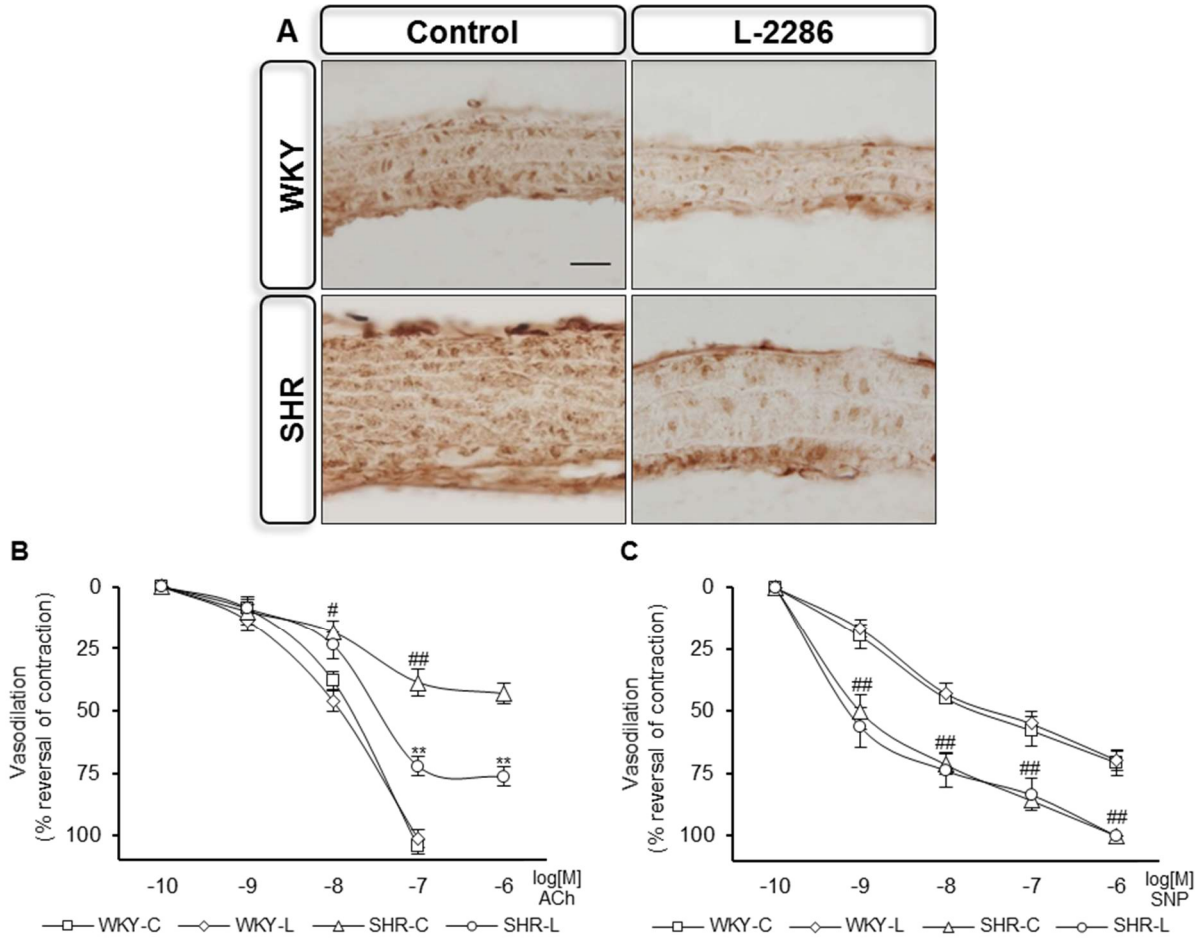

Figure 5.: The endothelial dysfunction and increased NT formation observed in carotid arteries of SHR animals were attenuated by L-2286 treatment. (A) Representative micrographs of immunostaining for NT accumulation in carotid arteries (scale bar 30 μm). (B, C) Relaxation properties of isolated carotid artery rings against 60 mM KCl pre-contraction, in the presence of cumulative doses of (B) ACh or (C) SNP. Data are presented as mean±S.E.M. $^{\#}p<0.05$, $^{\#\#}p<0.01$ vs. WKY-C; $^{**}p<0.01$ vs. SHR-C.

Next, we asked whether this beneficial effect may improve vasomotor properties of isolated carotid artery rings against 60 mM KCl pre-contraction, in the presence of increasing doses of ACh (Fig. 5B) or SNP (Fig. 5C). The externally evoked maximum contractile force of isolated CCA rings was similar across the groups. Cumulative response curves of CCA rings of the SHR and WKY strains became distinguishable at higher doses of ACh and, while 10^{-6} M ACh completely reversed KCl induced wall tension of CCA rings isolated from normotensive animals, this reduction was only partial for hypertensive control rats (strain factor.: $p<0.01$). 32 weeks of L-2286

treatment aided the preservation of endothelium-dependent relaxation capabilities to ACh administration of SHR-L CCA rings (SHR-L vs SHR-C, $p<0.01$).

SNP is a NO donor molecule and its effect is dependent on vSMC function. In the presence of the compound, CCA rings isolated from hypertensive rats demonstrated hyper-reactivity, even at lower doses (Fig. 5C). L-2286 treatment slightly modulated vasomotor responses of SHR-L CCAs for SNP administration, however, the effect was not statistically significant.

4.1.3. In carotid arteries of hypertensive rats, long-term L-2286 treatment mitigated AIF translocation and interfered with MAPK and NF-κB signaling

One of the most elaborated beneficial effects of PARP-1 activity modulation in acute stress situations is the reduced incidence of the necrotic form of cell death by signaling interference and cellular energy conservation or a bias towards apoptotic events, and in this way, serves in reducing the inflammation and genotoxic burden of surrounding tissues[61]. During chronic hypertension, reorganization of cellular-ECM associations and structural remodeling of the vasculature are accompanied by cell death events[3, 77]. Therefore, we evaluated in our chronic model, whether PARP-1 participates in these processes due to the oxidatively stressed environment. A hallmark of excess PARP-1 activity initiated cell death is the release of AIF from the mitochondrial inter-membrane space and its translocation to the nucleus to initiate DNA degradation[35]. By confocal microscopy, co-localization of the fluorophore-labeled AIF with the nuclear staining could be observed in a fraction of cellular components only within the control hypertensive group (Fig. 6C), but not in carotid arteries of L-2286 treated SHRs (Fig. 6D) or normotensive rats (Fig. 6A,B).

Hypertension induced phenotypic alterations of various vascular segments are in part, governed by inflammatory processes related to NF-κB function and an altered cellular physiology of vascular components, as the result of an oxidative and mechanical stress-driven bias in the activity of MAPK members. Previous data by our group demonstrated how modulating PARP-1 activity by pharmacological means or RNA interference during oxidative stress elevates the cellular level of MKP-1[67, 77]. Since this kinase is an important upstream regulator of various MAPK's activity, we hypothesized the modulation of the vascular remodeling processes may be connected

to an altered MAPK system regulation by long-term PARP-1 inhibition. Immunofluorescent labeling of MKP-1 in carotid arteries revealed an elevated expression in control hypertensive animals (Fig. 6G) relative to WKY groups (Fig. 6E,F), which was further increased in L-2286 treated SHRs (Fig. 6H).

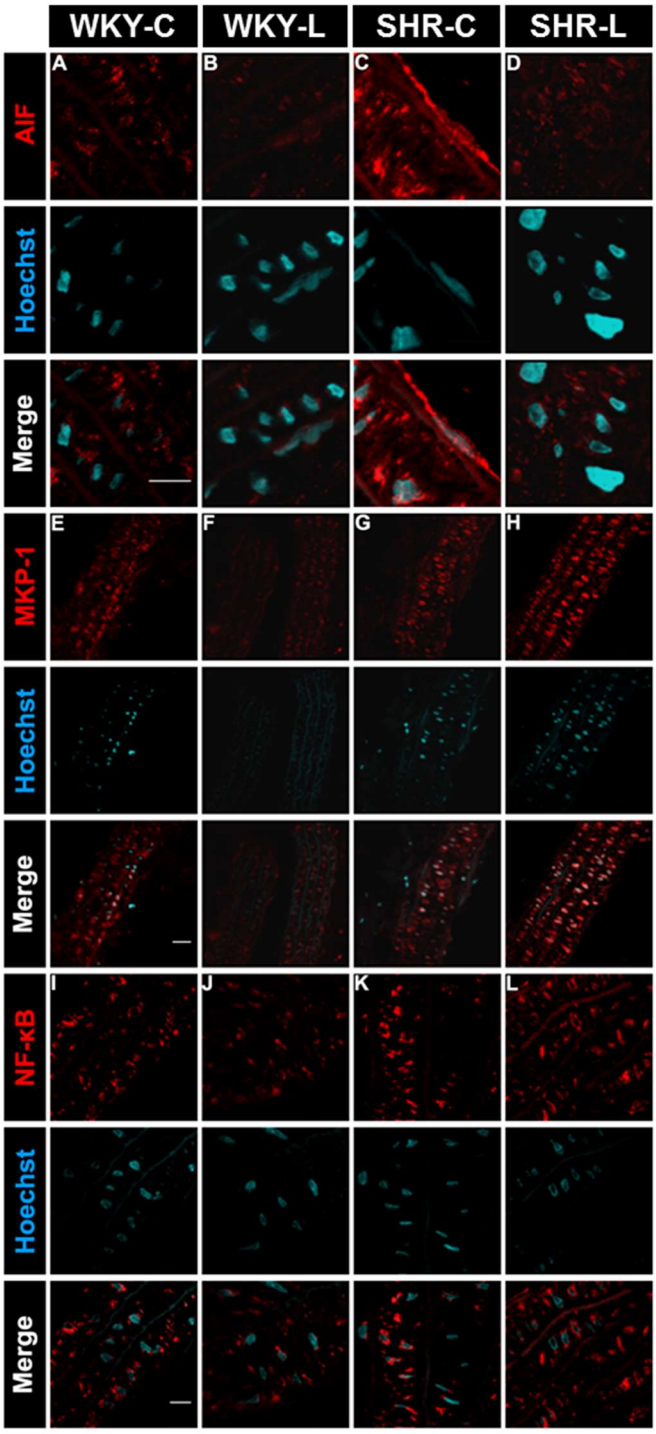

As PARP-1 is an important co-regulator of NF-κB in inflammatory processes[66] we assessed, whether pharmacological modulation of PARP-1 activity alters its cytoplasmic activation and nuclear activity. In carotid arteries of control hypertensive rats, a profound activation and nuclear translocation of NF-κB were observed (Fig. 6K) compared to the WKY groups, in which NF-κB could be found predominantly in the extranuclear compartment by confocal microscopy (Fig. 6I,J). The above process was substantially attenuated by long-term L-2286 administration in the carotid arteries of SHR animals (Fig. 6L).

Figure 6.: Fluorescent staining for AIF and NF-kB cellular distribution and MKP-1 expression. (A-D) Nuclear translocation of AIF in carotid artery walls of (A) WKY-C, (B) WKY-L, (C) SHR-C and (D) SHR-L animals (scale bar: 10 μm). (E-H) Cellular level of MKP-1 in (E) WKY-C, (F) WKY-L, (G) SHR-C and (H) SHR-L animals (scale bar: 25 μm). (I-L) Subcellular distribution of NF-kB in (I) WKY-C, (J) WKY-L, (K) SHR-C and (L) SHR-L animals (scale bar: 10 μm).

4.2. Specific Aim 2. Observation of chronic hypertension related alterations of the dorsal hippocampus in the SHR strain, focusing on the level of oxidative stress and cell death events.

4.2.1. Structural alterations of the dorsal hippocampus in the hypertensive animals

We sought to determine long-term effects of systemic L-2286 administration on target organ damage in the SHR model, focusing particularly on markers of oxidative stress and consequent damage of the neuronal tissue. For this purpose, the hippocampal area was a suitable model with easy localization, compactly ordered cell layers and expansive areas of fiber tracts.

On the macroscopic level, brains of the chronic hypertensive rats demonstrated a marked dilatation of cerebral ventriculi. On PAS stained sections, we observed consequences of this alteration regarding dorsal hippocampal structure in SHR animals (Fig. 7). The shortening of its mediolateral axis and deformation of gyrus dentatus with a flattened crest part was apparent, most likely be induced by the exerted pressure from the 3rd and lateral cerebral ventriculi. However, long term PARP-1 inhibition had no overt effects on these malformations in treated hypertensive rats, the structure of transverse vessels supplying the hippocampal region was more preserved compared to the irregular lumen shapes observed in the control SHR animals (Fig. 7).

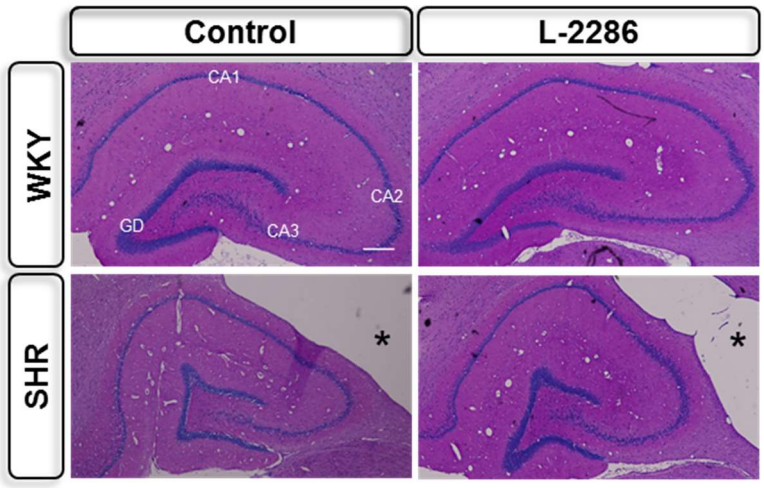

Figure 7. Chronic hypertension related structural alterations in the rat dorsal hippocampus. The dorsal hippocampus on PAS-stained sections of given groups (scale bar: 200 μm). GD, gyrus dentatus; CA1, cornu ammonis 1; CA2, cornu ammonis 2; CA3, cornu ammonis 3; * marks the lateral cerebral ventriculus

Notably, the presence of lacunar forms of perivascular white matter damage was sporadically present in the SHR-C animals. This alteration was absent in WKY animals and occurred to a much lesser extent in L-2286 treated SHRs (Fig. 9F).

4.2.2. Systemic L-2286 administration in SHR animals attenuated oxidative damage in the area of dorsal hippocampus

To assess levels of oxidative damage of lipoproteins and lipids, we labeled brain sections by NT (Fig. 8A) and 4-HNE (Fig. 8B) immunohistochemistry, respectively. During these observations, hypertension related accumulation of nitrated tyrosine residues and the increased peroxidation of lipid membranes were apparent in cellular components and fiber tracts of the hippocampal area of control SHRs. As a sign of attenuated ROS production, long-term L-2286 treatment lowered accumulation of both NT and 4-HNE products in this area of treated hypertensive rats.

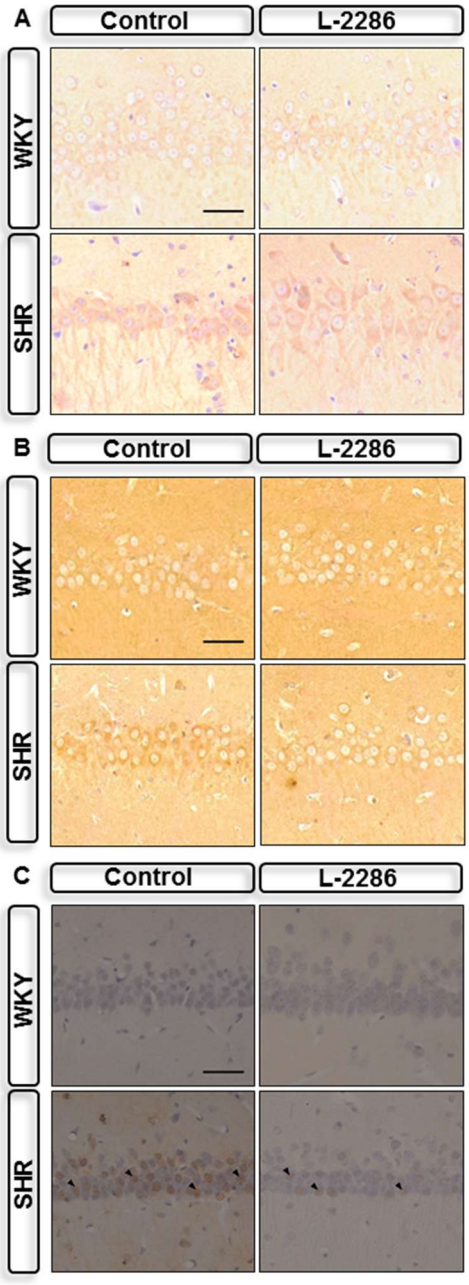

We also evaluated oxidants induced base-modifications of the DNA in pyramidal cells of the CA1 region by immunohistochemistry to visualize 8-oxoG products (Fig. 8C). In SHR-C animals, a higher portion of 8-oxoG labeled nuclei was observed compared to the normotensive groups in this area. The extent of oxidative DNA damage in pyramidal cells was attenuated by the applied treatment in SHR animals. Taken all together, in chronic hypertensive rats a substantially elevated level of oxidative stress was revealed in the dorsal hippocampal area, as a model for hypertension-

Figure 8. Long term L-2286 administration attenuated the oxidative damage of neuronal tissue. (A) NT and (B) HNE staining of CA1 regions for the evaluation of nitrosative damage and lipid peroxidation of pyramidal neurons, respectively, in the dorsal hippocampus (scale bar 50 μm). Representative micrographs of immunostaining for (C) 8-oxG (scale bar 50 μm), ► points to some positively labeled nuclei.

related damage of the neuronal tissue. This process and consequent damage of biomolecules were substantially attenuated by long-term pharmacological modulation of PARP-1 activity in SHR animals.

4.2.3. Long-term L-2286 administration attenuated pyramidal cell loss in the CA1 area of treated SHR animals

Next, we evaluated whether the increased level of oxidative stress and related DNA damage may lead to excess PARP-1 activation in the CA1 region of hypertensive animals. Immunohistochemistry was implemented to label the extent of poly(ADP-ribose)-polymer/PAR formation on brain slices (Fig. 9A). Delineating the results of 8-oxoG observations regarding oxidative damage of DNA (Fig. 8C), an elevated level of PAR polymer formation was found, with a typical marginal staining of the nuclei in CA1 pyramidal neurons of SHR animals relative to their normotensive counterparts. Long-term PARP-1 inhibition via L-2286 treatment resulted in a lowered intensity of PAR staining in treated animals of both strains.

We hypothesized the observed PARP-1 activation may initiate cell death events, therefore quantified pyramidal cell numbers on Cresyl violet stained sections in the CA1 region (Fig. 9B,C). The results revealed a marked atrophy of this area by a significantly lower cell number in SHR animals (strain factor: $p<0.01$). Pharmacological modulation of PARP-1 activity led to a more preserved cellular content of the CA1 region in hypertensive rats. To elucidate “on-going” processes of pyramidal cell loss, we applied the TUNEL-test on brain slices to mark nuclei with a fragmented DNA content (Fig. 9D). In this observation, the reduced CA1 cell number of hypertensive rats was accompanied by a higher fraction of TUNEL positive nuclei (strain factor: $p<0.01$) (Fig. 9E). While 32 weeks of L-2286 administration had no overt effect on cellular content or incidence of cell death events in the CA1 region of WKY animals, treated hypertensive rats demonstrated a more preserved status regarding these parameters (SHR-L vs SHR-C $p<0.01$) (Fig. 9D,E).

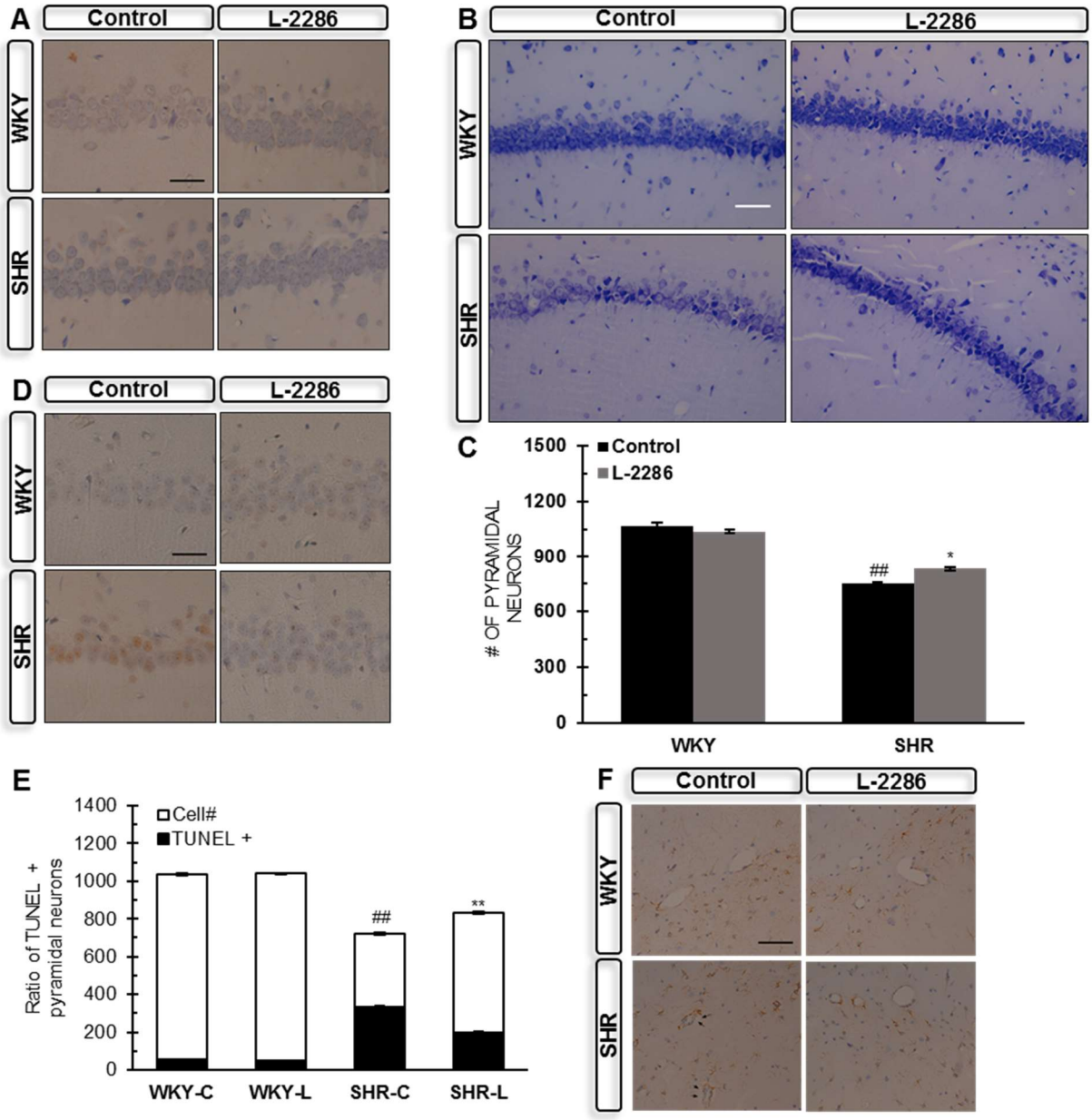

Figure 9. L-2286 administration attenuated PAR formation related cell loss and reactive astrogliosis observed in the dorsal hippocampus of SHR rats. (A) PAR polymer formation in the CA1 area of given groups (scale bar 50 μm). (B-C), (B) Representative micrographs of CA1 region of the dorsal hippocampus with Cresyl violet staining (scale bar 50 μm) and (C) quantitation of pyramidal cell numbers in the CA1 area. (D-E) Representative micrographs on the results of (D) TUNEL test (scale bar 50 μm) and (E) quantitation of TUNEL+ nuclei relative to total cell numbers of the CA1 region. (F) Representative micrographs on immunohistochemistry against GFAP to visualize the activated astroglia population (scale bar 50 μm), ►: perivascular lacunar forms of white matter damage. Data are presented as mean±S.E.M. ##p<0.01 vs. WKY-C; *p<0.05, **p<0.01 vs. SHR-C.

Astroglial activation in the neuronal tissue indicates a perturbative microenvironment, in which glial cells respond by an increase in their size (hypertrophy) or numbers (hyperplasia) to support functions of neurons or the endothelial cells forming the BBB[78]. We immunolabeled the intermediate-filament

GFAP to evaluate the perivascular distribution of this glial subpopulation (Fig. 9F). No profound difference was found in the number of astrocytes between the strains at the area of the hippocampal fissure, although an alteration in their size as a sign of hypertrophy and a pronounced perivascular immunoreactivity were observed in chronic hypertensive animals. 32 weeks of treatment by L-2286 reduced astroglia numbers in both strains with marginal effect on their reactive hypertrophy in SHR animals. The perivascular presence of reactive astrocytes was attenuated by applied treatment.

4.3. Specific Aim 3. To elucidate evidence of mitochondrial protection achieved by long-term PARP-1 inhibition in the myocardium.

4.3.1. Ultrastructural observations on the interfibrillar mitochondria population in the myocardium

Longitudinal sections were taken to evaluate the *status quo* of interfibrillar mitochondria on electron microscopic preparations in the myocardium of 42 weeks old SHRs, with or without L-2286 treatment. This subpopulation, packed compactly between the contractile elements, has a profound role in supplying the energy demand of cardiac work. This way, their dysfunction or disturbances in the processes

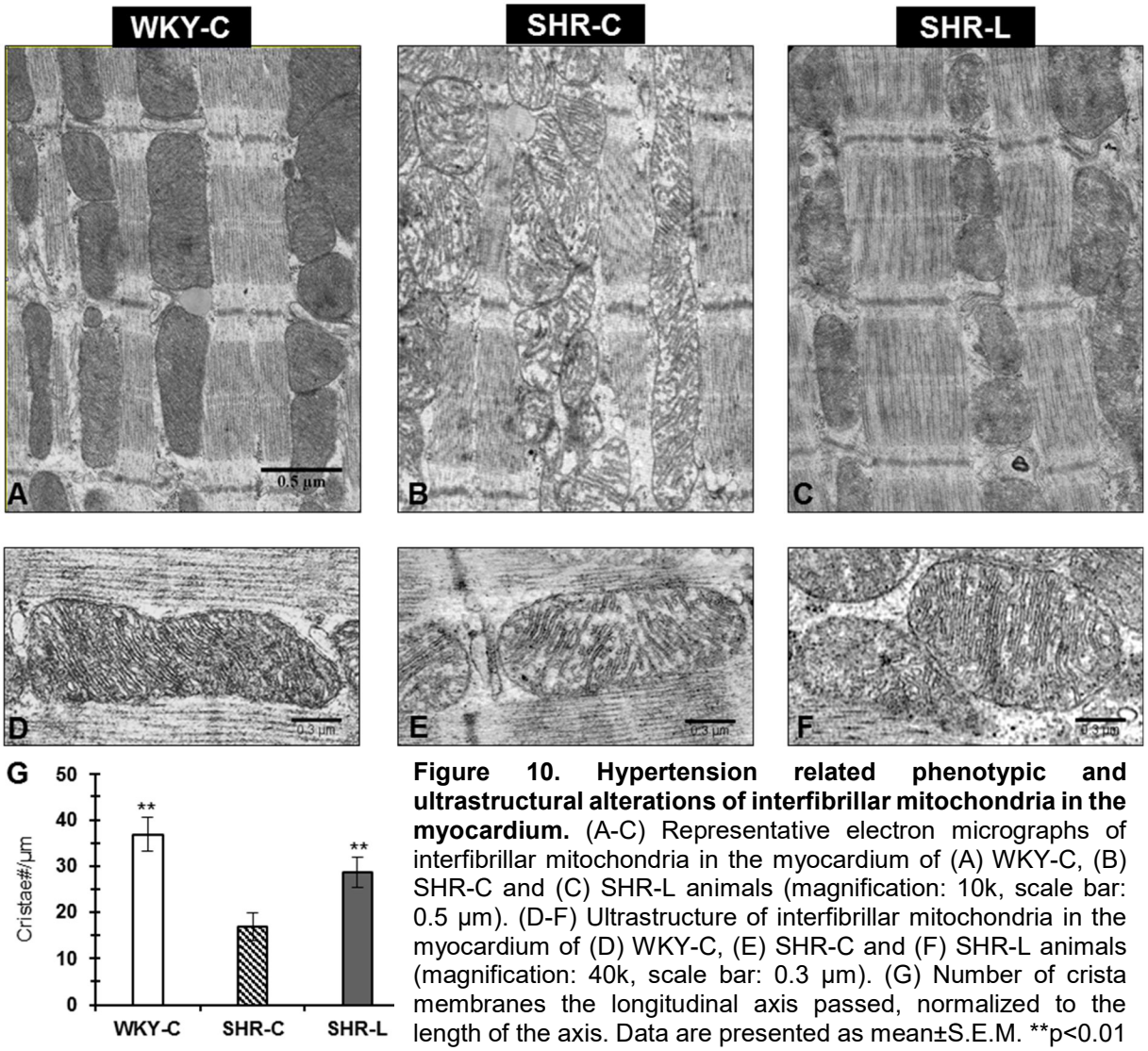

Figure 10. Hypertension related phenotypic and ultrastructural alterations of interfibrillar mitochondria in the myocardium. (A-C) Representative electron micrographs of interfibrillar mitochondria in the myocardium of (A) WKY-C, (B) SHR-C and (C) SHR-L animals (magnification: 10k, scale bar: 0.5 µm). (D-F) Ultrastructure of interfibrillar mitochondria in the myocardium of (D) WKY-C, (E) SHR-C and (F) SHR-L animals (magnification: 40k, scale bar: 0.3 µm). (G) Number of crista membranes the longitudinal axis passed, normalized to the length of the axis. Data are presented as mean±S.E.M. **p<0.01 vs. SHR-C.

maintaining network integrity may have fundamental roles during the evolution of cardiomyopathies[54].

In the SHR-C group (Fig. 10B), a morphologically more heterogeneous population was observed with partial loss of electron density in the mitochondrial matrices. These mitochondria were loosely packed between the myofilaments demonstrating an intensely disorganized picture relative to the WKY myocardium (Fig. 10A). Observing the mitochondrial inner membranous structures in normotensive animals we found the cristae to be densely packed, forming regular, wrinkled shapes (Fig. 10D). In contrast, the reduced number of inner membranes ($p<0.01$) and dilation of cristae spaces and junctions was apparent in control hypertensive rats (Fig. 10E,G). The myocardium of L-2286 treated SHR rats demonstrated an intermediate phenotype (Fig. 10C) with regional heterogeneity, yet a more preserved inner structure, (Fig. 10F) and cristae numbers of interfibrillar mitochondria ($p<0.01$) (Fig. 10G).

4.3.2. Quantifying the actual state of interfibrillar mitochondrial dynamics

In order to gain insight into the actual equilibrium of fusion-fission processes, we measured the area (Fig. 11A) and the length of the longitudinal axis (Fig. 11B) of interfibrillar mitochondria on electron micrographs (~500 mitochondria/group). The results issued a profound decrease in the mean mitochondrial area of SHR-C group with the shortening of longitudinal axes in comparison to WKY animals, suggesting a more fragmented phenotype in the hypertensive rats. The values of L-2286 treated SHRs differed significantly from the control hypertensive group regarding both mitochondrial areas ($p<0.01$) and the lengths of longitudinal axes ($p<0.01$). Next, we assessed relative frequencies of measured mitochondrial areas in arbitrary intervals of 0.3 μm^2 and found a transition towards the lowest interval in the SHR-C myocardium (Fig. 11C), where nearly half of measured mitochondria had an area lower than 0.3 μm^2. This skewness of area values was attenuated in treated SHR animals and, similar to the normotensive group, the majority of measured mitochondria featured area values above 0.3 μm^2.

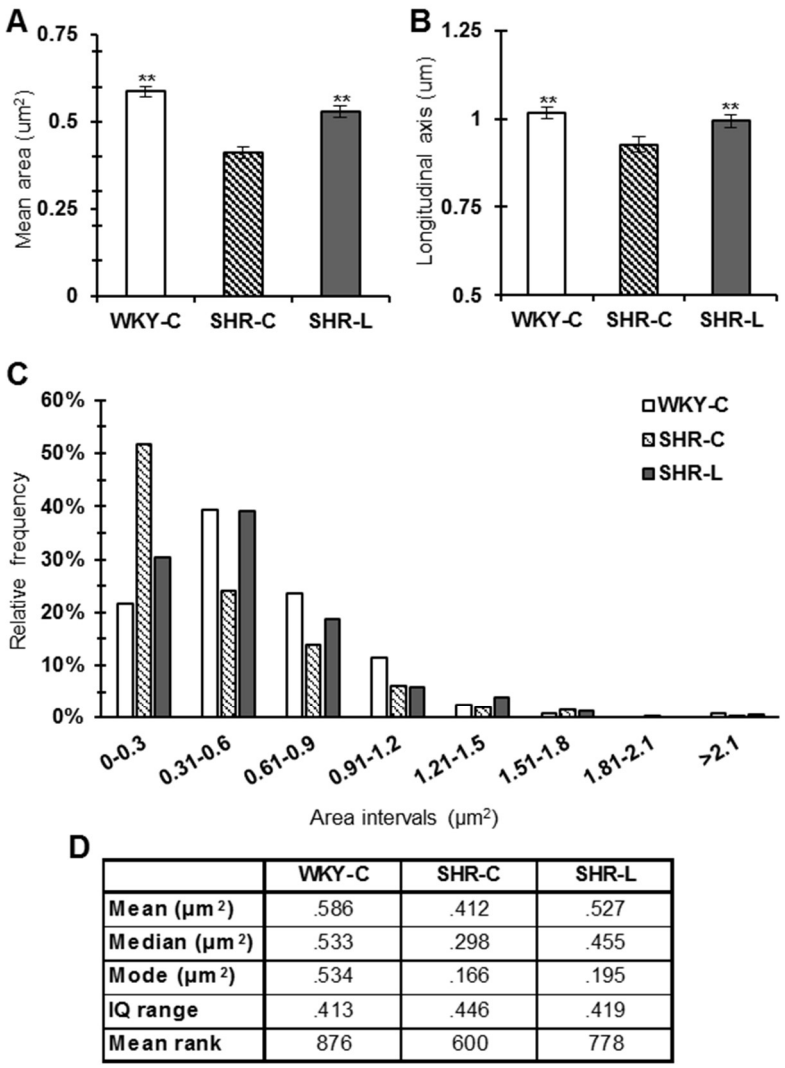

D

	WKY-C	SHR-C	SHR-L
Mean (µm²)	.586	.412	.527
Median (µm²)	.533	.298	.455
Mode (µm²)	.534	.166	.195
IQ range	.413	.446	.419
Mean rank	876	600	778

Figure 11. Hypertension related fragmentation of interfibrillar mitochondria in the myocardium. (A) Means of area values in given groups. (B) Mean length of the longitudinal axes. (C) Relative frequencies of measured mitochondrial areas in arbitrary intervals. (D) Central descriptors and interquartile range (IQ) of raw mitochondrial area measurements and the means of ranked values. Data are presented as mean±S.E.M. **p<0.01 vs SHR-C

4.3.3. Effects of L-2286 treatment on cellular levels and subcellular distributions of fusion-fission regulators.

We sought to determine levels of OPA1 and the fission mediator DRP1, in the myocardium in whole cell and fractionated Western blot samples, to gain insight at the molecular level of attenuated fission processes and preserved inner mitochondrial structures in treated hypertensive animals.

First, we assessed the efficacy of L-2286 treatment in whole cell preparations by the extent of auto-PARylation (Fig. 12A). The highest PAR-polymer formation was observed in control hypertensive animals in comparison to the low signal in the WKY group ($p<0.01$). L-2286 administration diminished the activity of PARP-1 in treated SHRs ($p<0.01$) (Fig. 12B).

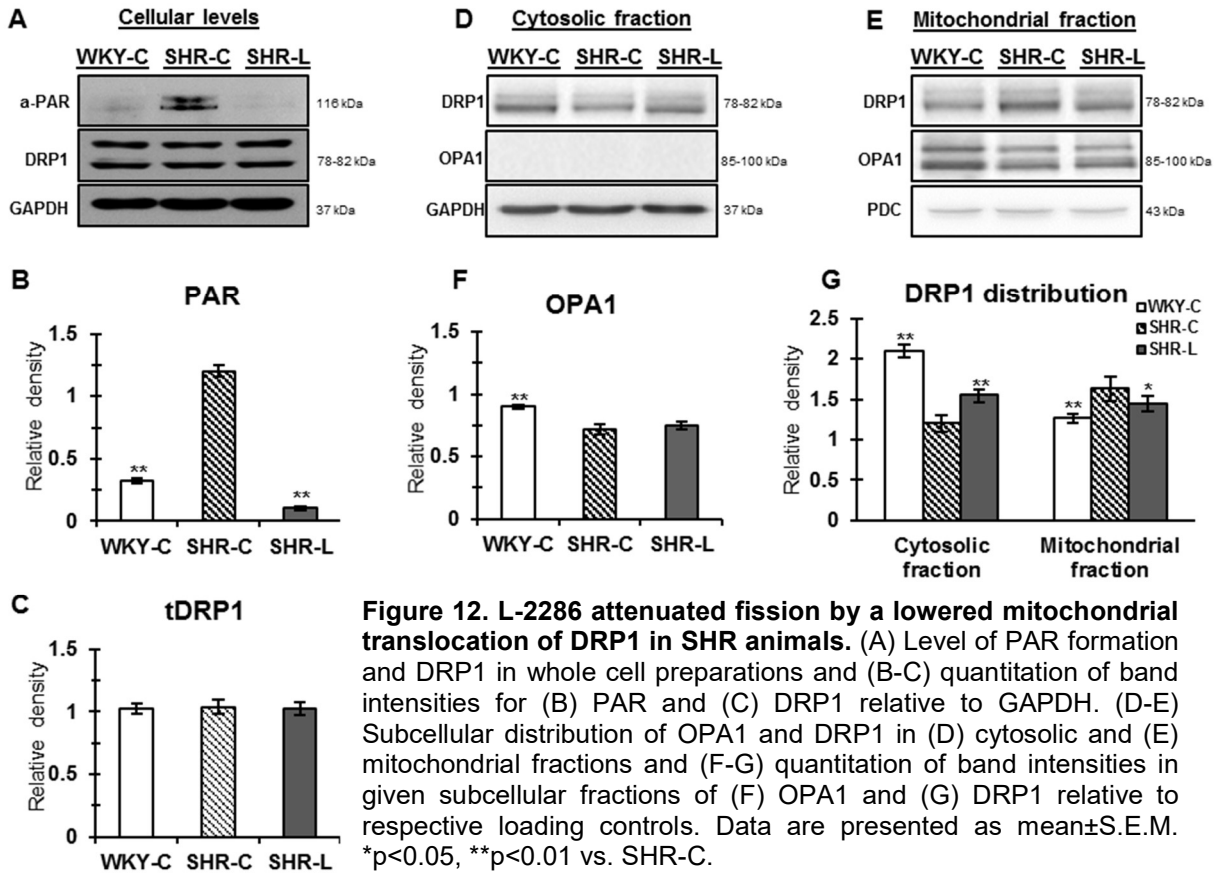

Figure 12. L-2286 attenuated fission by a lowered mitochondrial translocation of DRP1 in SHR animals. (A) Level of PAR formation and DRP1 in whole cell preparations and (B-C) quantitation of band intensities for (B) PAR and (C) DRP1 relative to GAPDH. (D-E) Subcellular distribution of OPA1 and DRP1 in (D) cytosolic and (E) mitochondrial fractions and (F-G) quantitation of band intensities in given subcellular fractions of (F) OPA1 and (G) DRP1 relative to respective loading controls. Data are presented as mean±S.E.M. *p<0.05, **p<0.01 vs. SHR-C.

In respect to DRP1, we found no overt differences in its cellular levels across the groups (Fig. 12A,C) although, when observing fractionated samples (Fig. 12D,E), a significantly higher portion was observed in mitochondrial fractions of SHR-C animals relative to normotensive controls ($p<0.01$), as a possible sign of accentuated translocation and anchorage to the OMM (Fig. 12G). Long-term PARP-1 inhibition in hypertensive rats resulted in the retention of a greater portion of DRP1 in the cytosolic fraction relative to SHR-C samples ($p<0.01$) (Fig. 12D), with a lowered translocation to mitochondria ($p<0.05$) (Fig. 12E). Cellular levels of OPA1 (Fig. 12E), regulating the integrity and fusion of inner mitochondrial membranes, was significantly reduced in hypertensive animals ($p<0.01$) with only a marginal elevation by L-2286 treatment, not reaching the level of statistical significance (Fig. 12F).

5. Discussion

At the age of 42 weeks, our results revealed profound differences in chronic hypertensive animals compared to their normotensive counterparts, regarding structural alterations of carotid arteries and the accumulation of oxidative biomarkers in the observed tissues. Although the applied L-2286 treatment did not exert a significant effect on the elevated blood pressure of SHR animals as the causative factor (Fig. 4A), it moderated structural and functional remodeling of carotid arteries, and also lowered the level of oxidative damage evaluated in the supplied tissues. Nitrative modification of lipoproteins by accentuated $ONOO^-$ formation was assessed by immunohistochemistry, at the level of carotid arteries (Fig. 5A) and the dorsal hippocampus (Fig. 8A). In the latter area of hypertensive rats, our research established enhanced levels of oxidative damage to lipid membranes visualized by 4-HNE staining (Fig. 8B), and oxidative base-modification of the DNA (Fig. 8B) in CA1 pyramidal neurons accompanied by elevated PAR formation (Fig. 9A) and cell loss (Fig. 9C, E). In the myocardium of SHR animals, a more fragmented phenotype of IFM (Fig. 11A, C) and activation of PARP-1 were demonstrated (Fig.12 B), as an indirect marker of elevated oxidative stress. These observations demonstrate, how in the SHR strain a hypertension-related enhancement of oxidative stress drives the pathological characteristics of target organ damage.

Cellular oxidative stress is the result of an insufficient antioxidant capacity in the face of boosted ROS production by various enzyme systems, including the mitochondrial ETC[2]. In the endothelial layer of carotid arteries and in perivascular areas of supplied tissues, O_2^- production, due to uncoupled eNOS and augmented NOX enzyme activity, confers deleterious effects by the diminished bioavailability of the potent vasodilator NO via $ONOO^-$ formation[3], inducing dysregulation of the vascular tone which further elevates the peripheral resistance and impairs blood supply of tissues[2, 3]. Additionally, $ONOO^-$ produced in the vicinity of the vascular endothelium is a potent activator of PARP-1 via its direct DNA-damaging properties[38, 40, 41]. As the result, endothelial dysfunction of carotid arteries isolated from hypertensive rats was observed by the impaired relaxation capabilities in the presence of ACh (Fig. 5B). Although the hyper-reactivity of SHR vessels to SNP was not affected by the long-term L-2286 administration in a significant manner (Fig. 5C), the endothelium-dependent

relaxation capability of isolated carotid arteries was more preserved in treated hypertensive animals accompanied by lowered NT accumulation (Fig. 5A). The above results indicate in which the NO production and response may be differentially altered in the cellular components of SHR carotid arteries, resembling previous observations in this model regarding the role of PARP-1 activation in the evolution of endothelial dysfunction [29, 79]. In the background, $ONOO^-$ mediated uncoupling of eNOS is proposed to form the basis of impaired NO production in the endothelial layer[3, 40], suggested by observations on the decreased level of its cofactor, BH4 in the plasma of SHRs [39].

The inflammatory status of the vasculature during hypertension[5, 17], indicated by the accentuated nuclear activity of NF-kB in carotid arteries of SHR animals (Fig. 6K), may further augment this process. Damage of the endothelial layer and deteriorated barrier function followed by activation of PARP-1 enhances the expression of pro-inflammatory mediators in the vasculature via NF-kB function[66]. In this regard, a bidirectional mechanism is probable, in which the NO produced by inducible NOS/iNOS augments $ONOO^-$ formation in the oxidatively stressed vasculature, which in turn leads to further PARP-1 activation followed by more deleterious consequences[43]. As an important activator of NF-kB and co-regulator for its transcriptional functions[66], PARP-1 also prolongs the nuclear activity of this inflammatory mediator by inhibiting its interaction with the nuclear export receptor chromosome region maintenance 1/CRM1 via PARylation[80], resulting in the nuclear retention of NF-kB, which process was moderated by L-2286 treatment (Fig. 6L). This vicious cycle increases the severity of inflammation and oxidative damage, therefore, its long-term pharmacologic modulation may have contributed to the lowered nitrative damage and endothelial protection observed in carotid arteries (Fig.5 A, B) and dorsal hippocampus of L-2286 treated hypertensive animals (Fig. 7; Fig. 8A). A growing body of data demonstrates in which PARP-1 inhibition attenuates the severity of vascular endothelial dysfunction and is even capable of reversing these processes[81, 82], although the preserved endothelium-dependent vasomotor response of SHR animals (Fig. 5B) in our study was not manifested in altered blood pressure (Fig. 4A). These beneficial effects of pharmacological PARP-1 activity modulation may also participate in the observed protection of neuronal tissue, partially based on preserved structure of the BBB, which has been demonstrated to be deteriorated in numerous pathologies via inflammatory and immunological processes accompanied by ROS generation[22-

[25,48]. Although applied treatment had no overt effects on the excess production of cerebrospinal fluid/CSF and hydrocephalus present in SHR animals, the endothelial protection by L-2286 administration was indicated by the preserved structure of transverse vessels in the hippocampal fissure (Fig. 7) and lowered perivascular presence of activated astroglia and lacunar white matter damage in treated hypertensive animals (Fig. 9F). The results above indicate, the protective mechanisms of PARP-1 inhibition in the chronic hypertensive model are not primarily related to altering the mechanical factors to lower vascular stretch or cardiac work demand in the face of elevated blood pressure or even the excess CSF production leading to structural alterations of the dorsal hippocampus (Fig. 7), but are most likely based on the attenuation of an aggravated cellular stress responses and tissue inflammation.

Our observations regarding the moderated thickening of carotid artery walls in the treated hypertensive group (Fig. 4B), despite an arterial pressure comparable to control SHR animals (Fig. 4A), further delineates the importance and plausibility of the signaling interference. An intriguing example is the elevated cellular levels of MKP-1 in carotid arteries of treated hypertensive group (Fig. 6H). Ang II potentiated ROS production, mechanical stress and growth factor signaling lead to activation of various members of MAPK signaling cascade initiating transcriptional programs resulting in proliferation, hypertrophic response and migration of vSMCs, collagen accumulation, initiation of cell death programs and inflammation in the stressed tissues[83]. Accordingly, increased activity of MAPK members was previously observed in the SHR aorta by immunoblot accompanied by the thickening of the vascular wall and fibrotic tissue accumulation, where collagen bundles even protruded into vascular lumen disrupting the endothelial layer[14]. MKP-1 has low expression in various tissues during basal conditions, however in stress scenarios, due to a negative feed-back loop, increased MAPK system activation leads to upregulated transcription of the *DUSP1* gene[77, 83]. Additionally, MAPK members regulate the protein stability and activity of MKP-1 via various mechanisms[83]. This way, the increased cellular level of MKP-1 in carotid arteries of SHR-C animals (Fig. 6G) compared to the normotensive groups is connected to MAPK system activation. Recent data demonstrate that during the cellular oxidative stress response, PARP-1 is a negative regulator of MKP-1 expression via its enzymatic activity[14, 67] by modulating the DNA binding of activating transcription factor-4/ATF4[77]. Therefore, the facilitated expression of MKP-1 observed in carotid arteries of L-2286 treated SHRs (Fig. 6H) presumably mediated the lowered

structural remodeling of these vessels by negative regulation of various MAPK members. Interestingly, in the carotid arteries of normotensive animals, long-term L-2286 administration exerted opposite effects (Fig. 6J), raising the possibility in which the negative regulation of MKP-1 expression may be connected to stress situations related excess activation of PARP-1. The above data indicate in which hypertension induced phenotypic changes of the vasculature might be beneficially modulated by the interference of NF-κB[66] and MAPK activation[2, 14, 83, 84].

In relation to pathological PARP-1 activation, the main source and target of excess ROS production are the mitochondria. In chronic hypertension, vascular alterations related impairment in blood-flow regulation leads to chronic ischemia and metabolic insufficiency of the supplied tissues, which also propagates secondary ROS production via mitochondrial sources[2]. Additionally, the arterial rarefaction in neuronal tissue[21] and the insufficient vascularization of hypertrophied myocardium during hypertensive remodeling further worsens the oxygen supply of tissues and the removal of metabolic waste products[49]. The fragmentation of the IFM reticulum (Fig. 11C), and the atrophic alteration of hippocampal cortices (Fig. 9C, E) accompanied by the presence of reactive astrogliosis (Fig. 9F) as an indicator of a metabolically perturbative environment observed in control hypertensive animals delineates these processes. Mitochondrial dysfunction and secondary ROS production are already established in numerous diseases characterized by oxidative stress-related PARP-1 activation in acute scenarios such as ischemia-reperfusion damage[85], also in chronic pathologies such as diabetes mellitus[86]. Positioned in the center of cellular stress response networks, it integrates signals via sensing the amount of DNA damage and as a target of various stress-responsive signaling routes of cytosolic or extracellular origin[60]. As the nuclear NAD+ bioavailability tightly regulates the activity of PARP-1 and its interaction with sirtuins, the actual metabolic status is capable of modulating the cellular stress response and *vice versa*[60, 87]. The output of these routes is cellular demise or survival via growth and compensatory mechanisms, depending on the amplitude and duration of stress.

The majority of responses determining cellular fate converge on the mitochondria, either in a direct or indirect manner. However, in acute versus prolonged stressful situations, different mechanisms may be dominant or present in various combinations. The original Berger's suicide model proposes, in which, during acute scenarios, the excess activation of PARP-1 by accumulating DNA damage depletes

nuclear NAD^+ pool, which eventually leads to a metabolic catastrophe[64], driving the cells towards a necrotic form of cell death instead of the well-controlled apoptotic route, which results in the spreading of cellular content, propagating inflammation and damage to bystander cells[35, 66]. Later studies established signaling properties of PAR polymers, detached from acceptor proteins. Translocated from the nucleus to mitochondria, it induces the release of the death effector AIF to initiate chromatin condensation. Further studies demonstrated the requirement of elevated intracellular Ca^{++} concentration and the activity of c-Jun N-terminal kinase/JNK in this process via facilitating permeabilization of the OMM[88]. In our study, the observed nuclear translocation of AIF by confocal microscopy in the carotid walls of control hypertensive rats (Fig. 6C), and also the higher incidence of pyramidal cell nuclei with fragmented DNA in the dorsal hippocampus of these animals (Fig. 9D, E) indicated “on-going” cell death events, which were profoundly attenuated by long-term pharmacological PARP-1 inhibition in these tissues. This effect possibly indicates various aspects of pharmacological PARP-1 inhibition in our chronic model. First, the energy conservation and attenuated cellular stress responses lower secondary ROS formation by protecting the mitochondria, indicated by lowered oxidative modifications of lipoproteins (Fig. 5A; Fig. 8A), lipids (Fig. 8B) and the DNA (Fig. 8C) in our observations. Particularly, in the neuronal tissue, which is heavily loaded with unsaturated fatty acids, protection of cellular membranes and myelin sheets against oxidative damage is vital for proper neuronal functions. The lowered oxidative status by treatment in our model also may facilitated cellular survival via compensatory mechanisms, this way foregoing the initiation of AIF-dependent cell death events. Additionally, via inhibited PAR formation, applied treatment may prevent nuclear-to-mitochondrial PAR signaling to induce AIF release[60]. Numerous studies indicate that pharmacological PARP inhibition in stressful situations results in the stabilization of OMM via AKT-1 activation[89] and, also may be capable of preventing its permeabilization by facilitating MKP-1 expression, this way attenuating activity MAPK death effectors, such as JNK and p38 MAPK (Fig. 2). As long-term L-2286 administration resulted in elevated MKP-1 expression in carotid walls of treated hypertensive rats (Fig. 6H), it further suggests the role of these mechanisms in mitochondrial protection in our chronic animal model. However, some recent results indicate the presence of an AIF subpopulation anchored to the cytosolic side of OMM, the translocation of which is sufficient to initiate nuclear events of parthanatos[90] hypothetically without the requirement of outer membrane permeabilization, above-

mentioned signaling mechanisms are established routes of mitochondrial protection by interfered PARP-1 activation[77, 85, 89]. Stabilization of the OMM in this way aids proper mitochondrial function and may have contributed to the attenuated secondary ROS formation in treated animals.

A somewhat less elucidated aspect of PARP-1 biology, in relation to mitochondrial dysfunction, is the presence of the PARP-1 enzyme in the mitochondrial matrix. Due to the potential technical difficulties and the discrepancy of results originating from different cellular model systems[91], it is challenging to consolidate overall conclusions on the relevance of this phenomenon, although PAR polymer formation in mitochondrial fractions was already demonstrated by several studies in the past decades[92]. Recently, Amati and his group indicated, in which PARP-1 is translocated from the nucleus to the mitochondrial matrix and this process required an interaction with Mitofilin[93]. The function of mitochondrial PARP-1 was advocated in the maintenance of mitochondrial genome integrity and gene expression. Additionally, PARylation and consequent inhibition of various ETC members and rate-limiting enzymes of the mitochondrial metabolism were demonstrated[91]. Based upon these data, Hungarian PARPologists proposed a working hypothesis, in which pathological activation of nuclear and mitochondrial PARP-1 in stressful situations occurs in tandem, leading to metabolic insufficiency, mitochondrial dysfunction and secondary ROS production[91]. This mechanism may advance our comprehensive understanding in respect to the role of PARP-1 effects on mitochondrial homeostasis, in addition to the above-mentioned stress signaling routes and the effects on nuclear NAD^+ metabolism.

We sought to take qualitative and quantitative assessments on the ultrastructural level regarding the actual state of the cardiac IFM network in the chronic hypertensive rat model. In the electron microscopic preparations, we obtained only a “snap-shot” of these highly dynamic processes defining the actual mitochondrial reticulum structure. However, quantification of individual mitochondrial areas demonstrated a robust alteration in the hypertrophied myocardium of SHR animals, including a shift towards a more fragmented phenotype (Fig. 11C). One must be cautious when interpreting this sole observation, as accentuated mitochondrial fragmentation is possibly the indicator of various processes and environmental conditions. Mitochondrial fission is the primary mechanism to segregate damaged organelles or to limit effects of various stressors to individual mitochondria, and in this

way, mitigates the propagation of damaging effects across the entire reticulum. The separated mitochondria face various destinies based upon the amount of received damage[54]. If it is cable of reconstituting its transmembrane potential, as an indicator of viable functions, it grows by importing proteins and various constituents to finally re-associate with the reticulum via the fusion mechanism. OPA1, mediating the fusion of inner mitochondrial membranes, has been demonstrated to have an important regulatory role during these processes. Dissipation of the mitochondrial transmembrane potential induces degradation of OPA1 by proteolytic cleavage[37, 94], and prevents re-association of the non-viable mitochondrion with the reticulum, which is designated to be eliminated via the mitochondria-specific autophagic process, defined as mitophagy[36, 37]. Our observation regarding the reduced levels of OPA1 in the hypertrophic myocardium (Fig. 12E, F) suggests the presence of mitochondrial damages, consonant with other studies revealing altered levels of fusion mediators in various cardiomyopathies[54]. However, long-term L-2286 treatment resulted in a trend toward higher levels of OPA1 compared to values of SHR-C animals, the induced difference was not statistically significant, and in this way, other mechanisms must have contributed to the more preserved picture of mitochondrial inner membranes in treated animals. As an example, excess translocation of DRP1 to the mitochondria is capable of inducing the remodeling of cristae membranes in a Ca^{++} dependent manner via an unknown mechanism, which is also required for the release of death effectors during initiation of cell death programs accompanied by mitochondrial fragmentation[37, 54].

As the above mechanisms suggest, mitochondrial fragmentation is an important step in the mitochondrial quality control as it's a prerequisite for mitochondrial biogenesis, also, the elimination via mitophagy[95]. These processes may form a partial explanation for the observed regional heterogeneity of mitochondria in the myocardium of SHR animals (Fig. 10C). However, inhibiting mitochondrial fission during acute stress scenarios, such as ischemia-reperfusion induced cardiac damage, is proved to be beneficial to protect cardiac muscle by limiting the necrotic area and aiding to preserve cardiac function in various models[37, 54], a long-term suppression of fission may carry deleterious consequences by interfering with processes of mitochondrial quality control[36, 95]. The same statement holds for the chronic, radical modulation of fusion processes in the myocardium, as the association of individual mitochondria is a primary means for changing metabolites and other mitochondrial constituents, also

required for the complementation of the mitochondrial genome in the case of mtDNA damage. In this manner, propagating hyper-fusion of mitochondria in chronic pathologies may lead to the accumulation of damaged mtDNA and other constituents in the entire mitochondrial reticulum, by preventing the separation of damaged portions resulting in dysfunction of the mitochondrial population[36]. This way in chronic models as the SHR, regarding mitochondrial protection the primary approach may likely be to modulate inducers of the pathological alterations, such as the prevention of secondary ROS generation in the stressed myocardium and stabilization of OMM to maintain a functional equilibrium of fusion/fission processes. Notably, these mechanisms first and foremost, possibly contributed to the lowered fragmentation of IFM by L-2286 treatment.

In addition to the presence of oxidative stress, other processes may participate in accentuated mitochondrial fragmentation observed in the hypertrophic myocardium. GTPase activity and mitochondrial translocation of DRP1 are regulated via various posttranslational modifications of the enzyme. Amongst these, DRP1 has been demonstrated to be constitutively phosphorylated by AMP-dependent protein kinase/PKA on a serine residue at the 637th position. This modification takes place in the GTPase effector domain of DRP1 and thought to maintain an inhibitory state[55]. Conversely, DRP1 at S637 is dephosphorylated by calcineurin, the activity of which has been demonstrated to increase during the hypertrophic response driven various pathologic alterations in relation to elevated intracellular Ca^{++} levels[96]. Attenuating the hypertrophic response in itself may help to preserve mitochondrial energy production and morphology. Furthermore, cellular metabolism and mitochondrial morphology seem to be mutually regulated in various studies during hyperglycemic insults or hypoxia and starvation[56]. Differentiated cardiomyocytes preferentially oxidize fatty acids for energy production, which is responsible for 60-80% of ATP production in the healthy myocardium, and to a lesser extent utilizes glucose, lactate, and ketone bodies. However, the ischemic condition of the hypertrophied myocardium, due to its insufficient vascularization following the thickening of the cardiac wall[49], would prefer additional glucose utilization for its higher ATP yield per oxygen molecule. The impaired capability of cardiac mitochondria to adapt to these changes during the hypertrophic response is a major contributor to the progression of cardiomyopathies and the transition of these conditions to overt heart failure[97]. Mechanistically, the accentuated nuclear NAD^+ catabolism, due to excess PARP-1 activation, may be

connected to the cardiac metabolic inflexibility in chronic scenarios. A great body of data demonstrates a functional interplay PARP family members and various sirtuins based on their common substrate usage[60]. For the purpose of the current discussion, the interplay between PARP-1 and SIRT1 having the uppermost importance[63]. These nuclear enzymes compete for NAD^+ availability as it limits their enzymatic activity[60], and for the physical interplay with nicotinamide mononucleotide adenylyltransferase 1/NMNAT1 which catalyzes the final reaction of the NAD^+ salvage pathway for its reconstitution, aiding their enzymatic functions[98, 99]. Furthermore, the by-product of their enzymatic reactions, nicotinamide, mutually inhibits their activity, also reciprocal posttranslational modifications have been revealed between these enzymes, a mechanism for their competition[60, 62]. In this fashion, the excess activation of PARP-1 in the stressed myocardium possibly limits functionality of SIRT1 with respect to regulation of peroxisome proliferator-activated receptor c coactivator 1/PGC1α. As a result, impairments of various processes of mitochondrial homoeostasis may emerge[63, 100], such as in biogenesis, substrate specificity and metabolic activitiy, and also in processes of mitochondrial ROS detoxification[97, 101]. Hypothetically, pharmacological inhibition of PARP-1 may help to alleviate impairment in the stressed tissues, this way aiding the metabolic fitness of cardiac mitochondria forming yet another explanation regarding the more preserved phenotype of IFM in treated SHRs. Although this latter mechanism was not directly evaluated in the current work, it likely supports the possibility of improving mitochondrial functionality via modulation of PARP-1 activity[63, 87, 100].

Comprehensively speaking, in the chronic hypertensive rat model, long-term pharmacological PARP-1 inhibition via systemic L-2286 administration without affecting arterial blood pressure, profoundly moderated hypertensive target organ damage via an attenuated level of oxidative stress, driving the pathological characteristics of the observed tissues in SHR animals. This effect is primarily based on mitochondrial protection via metabolic stability, attenuated cellular stress responses and additional signaling interference of inflammatory processes and the activity of MAPK members, regulating a plethora of cardiovascular pathological alterations during chronic hypertension. It led to a more preserved status in the observed tissues, accompanied by protected cellular content.

6. Novel findings

- Long-term L-2286 administration moderated the processes of hypertension-induced vascular remodeling regarding wall thickening and fibrotic tissue accumulation at the level of carotid arteries, demonstrated for the first time in the SHR model.
- Pharmacological modulation of PARP-1 activity attenuated the additional ROS and $ONOO^-$ formation in the stressed vasculature and neuronal tissue. Additionally, the applied treatment interfered in the stress-related activation of MAPK and NF-kB signaling routes, forming the molecular basis of attenuated structural and functional remodeling of the carotid arteries, without lowering the SBP.
- Applied treatment beneficially affected functionality and integrity of the endothelial layer in carotid arteries of hypertensive animals, and also protected the integrity of BBB in neuronal tissue indicated by the lowered perivascular presence of activated astrocytes in the area of the dorsal hippocampus. These effects and modulated activation of PARP-1 contributed to the more preserved cellular content in the observed tissues.
- A more fragmented phenotype of cardiac IFM and a disorganized inner structure were observed in hypertensive animals, which alterations were moderated by long term administration of L-2286. Applied treatment did not exert a significant effect on cellular levels of the fission and fusion regulators DRP1 and OPA1, respectively, however, it attenuated the mitochondrial translocation of DRP1 in hypertensive rats.

7. Publications of the author

(Cumulative impact factor: 30.622)

7.1. Relevant publications:

Krisztian Eros, Klara Magyar, Laszlo Deres, Arpad Skazel, Adam Riba, Zoltan Vamos, Tamas Kalai, Ferenc Gallyas Jr, Balazs Sumegi, Kalman Toth, Robert Halmosi:
Chronic PARP-1 Inhibition Reduces Carotid Vessel Remodeling and Oxidative Damage of the Dorsal Hippocampus in Spontaneously Hypertensive Rats.
PLOS ONE 12:(3) Paper e0174401. 18 p. (2017) **IF: 2.806**

Klara Magyar, Laszlo Deres, **Krisztian Eros**, Kitti Bruszt, Laszlo Seress, Janos Hamar, Kalman Hideg, Andras Balogh, Ferenc Gallyas Jr., Balazs Sumegi, Kalman Toth, Robert Halmosi:
A Quinazoline-derivative Compound with PARP Inhibitory Effect Suppresses Hypertension-induced Vascular Alterations in Spontaneously Hypertensive Rats.
BIOCHIM BIOPHYS ACTA Jul;1842(7):935-44 (2014) **IF:4.882**

7.2. Additional publications:

Agnes Kemeny, Katalin Cseko, Istvan Szitter, Zoltan Varga, Peter Bencsik, Krisztina Kiss, Robert Halmosi, Laszlo Deres, **Krisztian Eros**, Aniko Perkecz, Laszlo Kereskai, Laszlo Terezia, Tamas Kiss, Peter Ferdinandy, Zsuzsanna Helyes:
Integrative characterization of chronic cigarette smoke-induced cardiopulmonary comorbidities in a mouse model
***ENVIRON POLLUT*.** pii: S0269-7491(16)31444-0 (2017) **IF:5.099**

Eniko Hocsak, Viktor Szabo, Nikoletta Kalman, Csenge Antus, Anna Cseh, Katalin Sumegi, **Krisztian Eros**, Zoltan Hegedus, Ferenc Gallyas Jr, Balazs Sumegi, Boglarka Racz:
PARP Inhibition Protects Mitochondria and Reduces ROS Production via PARP-1-ATF4-MKP-1-MAPK Retrograde Pathway.
FREE RADICAL BIOLOGY AND MEDICINE 108:770-784 (2017) **IF: 5.606**

Adam Riba, Laszlo Deres, **Krisztian Eros**, Aliz Szabo, Klara Magyar, Balazs Sumegi, Kalman Toth, Robert Halmosi, Eszter Szabados:
Doxycycline Protects Against ROS-induced Mitochondrial Fragmentation and ISO-Induced Heart Failure
***PLOS ONE* 12**:(4) Paper e0175195. 16 p. (2017) **IF: 2.806**

Robert Halmosi, Laszlo Deres, Roland Gal, **Krisztian Eros**, Balazs Sumegi, Kalman Toth:
PARP Inhibition and Postinfarction Myocardial Remodeling.
INTERNATIONAL JOURNAL OF CARDIOLOGY 217:pp. S52-S59. (2016) **IF: 6.189**

Laszlo Deres, Eva Bartha, Anita Palfi, **Krisztian Eros**, Adam Riba, Janos Lantos, Tamas Kalai, Kalman Hideg, Balazs Sumegi, Ferenc Gallyas Jr., Kalman Toth, Robert Halmosi:
PARP-inhibitor Treatment Prevents Hypertension Induced Cardiac Remodelling by Favourable Modulation of Heat Shock Proteins, Akt-1/GSK-3β and Several PKC Isoforms.
PLOS ONE Jul 11;9(7):e102148 (2014) **IF:3.234**

7.3. Published abstracts:

Laszlo Deres, Klara Magyar, Imre Takacs, **Krisztian Eros**, Andras Balogh, Kalman Hideg, Balazs Sumegi, Kalman Toth, Robert Halmosi:
Pharmacological PARP-inhibition Decreases Vascular Fibrosis in Spontaneously Hypertensive Rat Model; *Congress of Hungarian Society of Cardiology 2012. Balatonfüred, Hungary. Cardiologia Hungarica 2012; 42:A21*

Laszlo Deres, Zoltan Vamos, **Krisztian Eros**, Robert Matics, Peter Cseplo, Robert Halmosi, Balazs Sumegi, Kalman Toth, Akos Koller:
Subcellular Aspects of AT1-receptor Mediated Vasomotor Responses in Relation to Age; *Congress of Hungarian Society of Cardiology 2013 Balatonfüred, Hungary. Cardiologia Hungarica 2013; 43:B16*

Krisztian Eros, Laszlo Deres, Klara Magyar, Adam Riba, Kalman Hideg, Laszlo Seress, Balazs Sumegi, Kalman Toth, Robert Halmosi:
Effect of PARP-1 Inhibition on the Mitochondrial Fragmentation in an *in vivo* SHR Model. *Congress of Hungarian Society of Cardiology 2013. Balatonfüred, Hungary*. *Cardiologia Hungarica 2013; 43:B16*

Zoltan Vamos, Laszlo Deres, **Krisztian Eros**, Robert Matics, Ivan Ivic, Andrea Bertalan, Elemer Sipos, Akos Koller, Peter Cseplo:
Age Related Changes of AT1 Receptor Mediated Vasomotor Responses in Isolated Rat Carotid Arteries. *Congress of Hungarian Society of Cardiology 2013. Balatonfüred, Hungary. Cardiologia Hungarica 2013; 43:B32*

Krisztian Eros, Laszlo Deres, Klara Magyar, Adam Riba, Kalman Hideg, Laszlo Seress, Balazs Sumegi, Kalman Toth, Robert Halmosi:
Effect of PARP-1 Inhibition on the Mitochondrial Fragmentation in an in vivos SHR Model. *VII. International Symposium on Myocardial Cytoprotection 2013 Pecs, Hungary. Cardiologia Hungarica 2013; 43:G12*

Robert Halmosi, Laszlo Deres, **Krisztian Eros**, Klara Magyar, Eva Bartha, Andrea Takacs, Tamas Kalai, Laszlo Seress, Ferenc Gallyas, Balazs Sumegi, Kalman Toth:
The Protective Effect of PARP-inhibitors Against Hypertension Induced Myocardial and Vascular Remodeling. *VII. International Symposium on Myocardial Cytoprotection 2013 Pecs, Hungary. Cardiologia Hungarica 2013; 43:G15*

Klara Magyar, Andrea Takacs, Laszlo Deres, **Krisztian Eros**, Laszlo Seress, Zoltan Vamos, Kalman Hideg, Tamas Kalai, Andras Balogh, Akos Koller, Balazs Sumegi, Kalman Toth, Robert Halmosi:

Pharmacological Inhibition of PARP-1 Enzyme Prevents Hypertensive Vascular Remodeling. *VII. International Symposium on Myocardial Cytoprotection 2013 Pecs, Hungary. Cardiologia Hungarica 2013; 43:G20*

Krisztian Eros, Eva Bartha, Laszlo Deres, Adam Riba, Tamas Kalai, Kalman Hideg, Balazs Sumegi, Kalman Toth, Robert Halmosi:
Effects of Poly(ADP-ribose)polymerase-1 Inhibition on Myocardial Remodeling in a Chronic Hypertensive Rat Model. *Congress of Hungarian Society of Cardiology 2014. Balatonfüred, Hungary. Cardiologia Hungarica 2014; 44:E51*

Laszlo Deres, **Krisztian Eros**, Noemi Bencze, Laszlo Seress, Balazs Sumegi, Sandor Farkas, Kalman Toth, Robert Halmosi:
The Effects of a Bradykinin B1 Receptor Antagonist on the Development of Hypertensive Organ Damages in SHR Model. *Congress of Hungarian Society of Cardiology 2014. Balatonfüred, Hungary. Cardiologia Hungarica 2014; 44:E25*

Laszlo Deres, **Krisztian Eros**, Noemi Bencze, Laszlo Seress, Balazs Sumegi, Sandor Farkas, Kalman Toth, Robert Halmosi:
The Effects of a Bradykinin B1 Receptor Antagonist on the Development of Hypertensive Organ Damages in SHR Model. *Congress of the European Society of Cardiology 2014. Barcelona, Spain. European Heart Journal (2014) 35 (Abstract Supplement), 664-665.*

Istvan Szitter, Robert Halmosi, Laszlo Deres, **Krisztian Eros**, Krisztina Kiss, Peter Bencsik, Zoltan V. Varga, Peter Ferdinandy, Zsuzsanna Helyes:
Predictive Mouse Model of Chronic Cigarette Smoke-Induced Pulmonary and Cardiac Pathophysiological Alterations. *Joint Meeting of the Federation of European Physiological Societies (FEPS) and the Hungarian Physiological Society 2014. Budapest, Hungary. Acta Physiol (Oxf) 2014 Aug;211 Suppl 697:1-184, Page 106: P5.10.*

Peter Jakus, Nikoletta Kalman, Fruzsina Fonai, Zoltan Hegedus, **Krisztian Eros**, Peter Dombovari, Balazs Sumegi, Balazs Veres:
Cyclophilin D-Dependent mPT Amplifies Inflammatory Response in Septic Shock. *5th World Congress on Targeting Mitochondria, 2014. Berlin, Germany. World Mitochondria Society Abstracts Book, Page 177.*

Adam Riba, Laszlo Deres, **Krisztian Eros**, Balazs Sumegi, Kalman Toth, Robert Halmosi, Eszter Szabados:
Protective Effect of Doxycycline Against the Development of Isoproterenol Induced Heart Failure. *Congress of Hungarian Society of Cardiology 2015. Balatonfüred,*

Hungary. CARDIOLOGIA HUNGARICA 45:(Suppl. D) p. D38. (2015)

Laszlo Deres, **Krisztian Eros**, Istvan Szitter, Peter Bencsik, Zoltan Varga, Peter Ferdinandy, Kalman Toth, Zsuzsanna Helyes, Robert Halmosi:
The Effects of Chronic Cigarette Smoke Inhalation on Cardiac and Pulmonary Function in Mice. *Congress of Hungarian Society of Cardiology 2015. Balatonfüred, Hungary. CARDIOLOGIA HUNGARICA 45:(Suppl. D) p. D46. (2015)*

Krisztian Eros, Arpad Skazel, Klara Magyar, Laszlo Deres, Kalman Hideg, Laszlo Seress, Balazs Sumegi, Kalman Toth, Robert Halmosi:
Systemic PARP-1 Inhibition Attenuates Carotid Vessel Remodelling and Have Protective Effects on Dorsal Hippocampus in Spontaneously Hypertensive Rats. *Congress of Hungarian Society of Cardiology 2016. Balatonfüred, Hungary. CARDIOLOGIA HUNGARICA 46:(Suppl. F) Paper F59.*

Adam Riba, Laszlo Deres, Arpad Skazel, **Krisztian Eros**, Balazs Sumegi, Kalman Toth, Eszter Szabados, Robert Halmosi:
Effects of Resveratrol on Postinfarct Heart Failure in vivo. *Congress of Hungarian Society of Cardiology 2016. Balatonfüred, Hungary. CARDIOLOGIA HUNGARICA 46:(Suppl. F) Paper F43.*

Kalman Toth, Laszlo Deres, Klara Magyar, **Krisztian Eros**, Balazs Sumegi, Robert Halmosi:
Myocardial and Vascular Protection by PARP Inhibitors. *3rd European Section Meeting of the International Academy of Cardiovascular Sciences,*
October 1-4, 2016, Marseille, France.
CURRENT RESEARCH: CARDIOLOGY - EXPERIMENTAL CLINICAL 3: p. 90. (2016)

Krisztian Eros, Arpad Skazel, Klara Magyar, Laszlo Deres, Tamas Kalai, Laszlo Seress, Balazs Sumegi, Kalman Toth, Robert Halmosi:
Systemic PARP-1 Inhibition Attenuates Carotid Vessel Remodelling and Have Protective Effects on Dorsal Hippocampus in Spontaneously Hypertensive Rats. *3rd European Section Meeting of the International Academy of Cardiovascular Sciences, October 1-4, 2016, Marseille, France.*
CURRENT RESEARCH: CARDIOLOGY - EXPERIMENTAL CLINICAL 3: p. 108. (2016)

8. References

1. Chobanian, A.V. et al. Seventh report of the Joint National Committee on Prevention, Detection, Evaluation, and Treatment of High Blood Pressure. *Hypertension* **42**, 1206-52 (2003).
2. Rubattu, S. et al. Pathogenesis of target organ damage in hypertension: role of mitochondrial oxidative stress. *Int J Mol Sci* **16**, 823-39 (2014).
3. Staiculescu, M.C., Foote, C., Meininger, G.A. & Martinez-Lemus, L.A. The role of reactive oxygen species in microvascular remodeling. *Int J Mol Sci* **15**, 23792-835 (2014).
4. Staiculescu, M.C. et al. Prolonged vasoconstriction of resistance arteries involves vascular smooth muscle actin polymerization leading to inward remodelling. *Cardiovasc Res* **98**, 428-36 (2013).
5. Gonzalez, J., Valls, N., Brito, R. & Rodrigo, R. Essential hypertension and oxidative stress: New insights. *World J Cardiol* **6**, 353-66 (2014).
6. Griendling, K.K., Sorescu, D., Lassegue, B. & Ushio-Fukai, M. Modulation of protein kinase activity and gene expression by reactive oxygen species and their role in vascular physiology and pathophysiology. *Arterioscler Thromb Vasc Biol* **20**, 2175-83 (2000).
7. Okamoto, K. & Aoki, K. Development of a strain of spontaneously hypertensive rats. *Jpn Circ J* **27**, 282-93 (1963).
8. Aoki, K. in Essential Hypertension 2 (ed. Aoki, K.) 3-8 (Springer Japan, Tokyo, 1989).
9. Kawabe, K., Watanabe, T.X., Shiono, K. & Sokabe, H. Influence on blood pressure of renal isografts between spontaneously hypertensive and normotensive rats, utilizing the F1 hybrids. *Jpn Heart J* **19**, 886-94 (1978).
10. Conrad, C.H. et al. Myocardial fibrosis and stiffness with hypertrophy and heart failure in the spontaneously hypertensive rat. *Circulation* **91**, 161-70 (1995).
11. Bartha, E. et al. PARP inhibition delays transition of hypertensive cardiopathy to heart failure in spontaneously hypertensive rats. *Cardiovasc Res* **83**, 501-10 (2009).
12. Bing, O.H. et al. The spontaneously hypertensive rat as a model of the transition from compensated left ventricular hypertrophy to failure. *J Mol Cell Cardiol* **27**, 383-96 (1995).
13. Limas, C., Westrum, B. & Limas, C.J. The evolution of vascular changes in the spontaneously hypertensive rat. *Am J Pathol* **98**, 357-84 (1980).
14. Magyar, K. et al. A quinazoline-derivative compound with PARP inhibitory effect suppresses hypertension-induced vascular alterations in spontaneously hypertensive rats. *Biochim Biophys Acta* **1842**, 935-44 (2014).
15. Pravenec, M. et al. Genetic analysis of cardiovascular risk factor clustering in spontaneous hypertension. *Folia Biol (Praha)* **46**, 233-40 (2000).
16. Nabha, L., Garbern, J.C., Buller, C.L. & Charpie, J.R. Vascular oxidative stress precedes high blood pressure in spontaneously hypertensive rats. *Clin Exp Hypertens* **27**, 71-82 (2005).
17. Sun, L. et al. Inflammation of different tissues in spontaneously hypertensive rats. *Sheng Li Xue Bao* **58**, 318-23 (2006).
18. Sagvolden, T. et al. The spontaneously hypertensive rat model of ADHD--the importance of selecting the appropriate reference strain. *Neuropharmacology* **57**, 619-26 (2009).

19. Sabbatini, M. et al. The hippocampus in spontaneously hypertensive rats: an animal model of vascular dementia? *Mech Ageing Dev* **123**, 547-59 (2002).
20. Bailey, E.L. et al. Cerebral small vessel endothelial structural changes predate hypertension in stroke-prone spontaneously hypertensive rats: a blinded, controlled immunohistochemical study of 5- to 21-week-old rats. *Neuropathol Appl Neurobiol* **37**, 711-26 (2011).
21. Pires, P.W., Dams Ramos, C.M., Matin, N. & Dorrance, A.M. The effects of hypertension on the cerebral circulation. *Am J Physiol Heart Circ Physiol* **304**, H1598-614 (2013).
22. Kaiser, D. et al. Spontaneous white matter damage, cognitive decline and neuroinflammation in middle-aged hypertensive rats: an animal model of early-stage cerebral small vessel disease. *Acta Neuropathol Commun* **2**, 169 (2014).
23. Sabbatini, M., Strocchi, P., Vitaioli, L. & Amenta, F. The hippocampus in spontaneously hypertensive rats: a quantitative microanatomical study. *Neuroscience* **100**, 251-8 (2000).
24. Amenta, F., Tayebati, S.K. & Tomassoni, D. Spontaneously hypertensive rat neuroanatomy: applications to pharmacological research. *Ital J Anat Embryol* **115**, 13-7 (2010).
25. Li, Y. et al. Age-related changes in hypertensive brain damage in the hippocampi of spontaneously hypertensive rats. *Mol Med Rep* **13**, 2552-60 (2016).
26. Briones, A.M. & Touyz, R.M. Oxidative stress and hypertension: current concepts. *Curr Hypertens Rep* **12**, 135-42 (2010).
27. Crowley, S.D. The cooperative roles of inflammation and oxidative stress in the pathogenesis of hypertension. *Antioxid Redox Signal* **20**, 102-20 (2014).
28. Soysal, P. et al. Oxidative stress and frailty: A systematic review and synthesis of the best evidence. *Maturitas* **99**, 66-72 (2017).
29. Pacher, P., Mabley, J.G., Soriano, F.G., Liaudet, L. & Szabo, C. Activation of poly(ADP-ribose) polymerase contributes to the endothelial dysfunction associated with hypertension and aging. *Int J Mol Med* **9**, 659-64 (2002).
30. Pacher, P. et al. Endothelial dysfunction in aging animals: the role of poly(ADP-ribose) polymerase activation. *Br J Pharmacol* **135**, 1347-50 (2002).
31. He, F. & Zuo, L. Redox Roles of Reactive Oxygen Species in Cardiovascular Diseases. *Int J Mol Sci* **16**, 27770-80 (2015).
32. Dymkowska, D. [Oxidative damage of the vascular endothelium in type 2 diabetes - the role of mitochondria and NAD(P)H oxidase]. *Postepy Biochem* **62**, 116-126 (2016).
33. Nosalski, R., McGinnigle, E., Siedlinski, M. & Guzik, T.J. Novel Immune Mechanisms in Hypertension and Cardiovascular Risk. *Curr Cardiovasc Risk Rep* **11**, 12 (2017).
34. Fortuno, A. et al. Association of increased phagocytic NADPH oxidase-dependent superoxide production with diminished nitric oxide generation in essential hypertension. *J Hypertens* **22**, 2169-75 (2004).
35. Virag, L., Robaszkiewicz, A., Rodriguez-Vargas, J.M. & Oliver, F.J. Poly(ADP-ribose) signaling in cell death. *Mol Aspects Med* **34**, 1153-67 (2013).
36. Dorn, G.W., 2nd & Kitsis, R.N. The mitochondrial dynamism-mitophagy-cell death interactome: multiple roles performed by members of a mitochondrial molecular ensemble. *Circ Res* **116**, 167-82 (2015).
37. Ong, S.B. & Gustafsson, A.B. New roles for mitochondria in cell death in the reperfused myocardium. *Cardiovasc Res* **94**, 190-6 (2012).

38. Pacher, P., Beckman, J.S. & Liaudet, L. Nitric oxide and peroxynitrite in health and disease. *Physiol Rev* **87**, 315-424 (2007).
39. Li, H. et al. Reversal of endothelial nitric oxide synthase uncoupling and up-regulation of endothelial nitric oxide synthase expression lowers blood pressure in hypertensive rats. *J Am Coll Cardiol* **47**, 2536-44 (2006).
40. Pacher, P. & Szabo, C. Role of the peroxynitrite-poly(ADP-ribose) polymerase pathway in human disease. *Am J Pathol* **173**, 2-13 (2008).
41. Islam, B.U. et al. Pathophysiological Role of Peroxynitrite Induced DNA Damage in Human Diseases: A Special Focus on Poly(ADP-ribose) Polymerase (PARP). *Indian J Clin Biochem* **30**, 368-85 (2015).
42. Laursen, J.B. et al. Endothelial regulation of vasomotion in apoE-deficient mice: implications for interactions between peroxynitrite and tetrahydrobiopterin. *Circulation* **103**, 1282-8 (2001).
43. Walsh, S.K., English, F.A., Crocker, I.P., Johns, E.J. & Kenny, L.C. Contribution of PARP to endothelial dysfunction and hypertension in a rat model of pre-eclampsia. *Br J Pharmacol* **166**, 2109-16 (2012).
44. Renna, N.F., de Las Heras, N. & Miatello, R.M. Pathophysiology of vascular remodeling in hypertension. *Int J Hypertens* **2013**, 808353 (2013).
45. Intengan, H.D. & Schiffrin, E.L. Vascular remodeling in hypertension: roles of apoptosis, inflammation, and fibrosis. *Hypertension* **38**, 581-7 (2001).
46. Touyz, R.M., He, G., El Mabrouk, M. & Schiffrin, E.L. p38 Map kinase regulates vascular smooth muscle cell collagen synthesis by angiotensin II in SHR but not in WKY. *Hypertension* **37**, 574-80 (2001).
47. Yang, Y. & Rosenberg, G.A. Blood-brain barrier breakdown in acute and chronic cerebrovascular disease. *Stroke* **42**, 3323-8 (2011).
48. Ueno, M. et al. Blood-brain barrier is impaired in the hippocampus of young adult spontaneously hypertensive rats. *Acta Neuropathol* **107**, 532-8 (2004).
49. Dorn, G.W., 2nd. Apoptotic and non-apoptotic programmed cardiomyocyte death in ventricular remodelling. *Cardiovasc Res* **81**, 465-73 (2009).
50. Sawyer, D.B. et al. Role of oxidative stress in myocardial hypertrophy and failure. *J Mol Cell Cardiol* **34**, 379-88 (2002).
51. Ueno, M. et al. Blood-brain barrier disruption in the hypothalamus of young adult spontaneously hypertensive rats. *Histochem Cell Biol* **122**, 131-7 (2004).
52. Ritter, S., Dinh, T.T., Stone, S. & Ross, N. Cerebroventricular dilation in spontaneously hypertensive rats (SHRs) is not attenuated by reduction of blood pressure. *Brain Res* **450**, 354-9 (1988).
53. Osterholt, M., Nguyen, T.D., Schwarzer, M. & Doenst, T. Alterations in mitochondrial function in cardiac hypertrophy and heart failure. *Heart Fail Rev* **18**, 645-56 (2013).
54. Ong, S.B. et al. Mitochondrial-Shaping Proteins in Cardiac Health and Disease - the Long and the Short of It! *Cardiovasc Drugs Ther* **31**, 87-107 (2017).
55. Santel, A. & Frank, S. Shaping mitochondria: The complex posttranslational regulation of the mitochondrial fission protein DRP1. *IUBMB Life* **60**, 448-55 (2008).
56. Babbar, M. & Sheikh, M.S. Metabolic Stress and Disorders Related to Alterations in Mitochondrial Fission or Fusion. *Mol Cell Pharmacol* **5**, 109-133 (2013).
57. Twig, G., Hyde, B. & Shirihai, O.S. Mitochondrial fusion, fission and autophagy as a quality control axis: the bioenergetic view. *Biochim Biophys Acta* **1777**, 1092-7 (2008).

58. Marin-Garcia, J. & Akhmedov, A.T. Mitochondrial dynamics and cell death in heart failure. *Heart Fail Rev* **21**, 123-36 (2016).
59. Huang, A. & Koller, A. Endothelin and prostaglandin H2 enhance arteriolar myogenic tone in hypertension. *Hypertension* **30**, 1210-5 (1997).
60. Luo, X. & Kraus, W.L. On PAR with PARP: cellular stress signaling through poly(ADP-ribose) and PARP-1. *Genes Dev* **26**, 417-32 (2012).
61. Pacher, P. & Szabo, C. Role of poly(ADP-ribose) polymerase 1 (PARP-1) in cardiovascular diseases: the therapeutic potential of PARP inhibitors. *Cardiovasc Drug Rev* **25**, 235-60 (2007).
62. Luna, A., Aladjem, M.I. & Kohn, K.W. SIRT1/PARP1 crosstalk: connecting DNA damage and metabolism. *Genome Integr* **4**, 6 (2013).
63. Bai, P. et al. PARP-1 inhibition increases mitochondrial metabolism through SIRT1 activation. *Cell Metab* **13**, 461-8 (2011).
64. Berger, N.A. & Berger, S.J. Metabolic consequences of DNA damage: the role of poly (ADP-ribose) polymerase as mediator of the suicide response. *Basic Life Sci* **38**, 357-63 (1986).
65. Virag, L., Salzman, A.L. & Szabo, C. Poly(ADP-ribose) synthetase activation mediates mitochondrial injury during oxidant-induced cell death. *J Immunol* **161**, 3753-9 (1998).
66. Bai, P. & Virag, L. Role of poly(ADP-ribose) polymerases in the regulation of inflammatory processes. *FEBS Lett* **586**, 3771-7 (2012).
67. Racz, B. et al. Regulation of MKP-1 expression and MAPK activation by PARP-1 in oxidative stress: a new mechanism for the cytoplasmic effect of PARP-1 activation. *Free Radic Biol Med* **49**, 1978-88 (2010).
68. Walker, J.W., Jijon, H.B. & Madsen, K.L. AMP-activated protein kinase is a positive regulator of poly(ADP-ribose) polymerase. *Biochem Biophys Res Commun* **342**, 336-41 (2006).
69. Rodriguez-Vargas, J.M. et al. ROS-induced DNA damage and PARP-1 are required for optimal induction of starvation-induced autophagy. *Cell Res* **22**, 1181-98 (2012).
70. Rodriguez-Vargas, J.M. et al. Autophagy requires poly(adp-ribosyl)ation-dependent AMPK nuclear export. *Cell Death Differ* **23**, 2007-2018 (2016).
71. Kulcsar, G. et al. Synthesis and study of new 4-quinazolinone inhibitors of the DNA repair enzyme poly(ADP-ribose) polymerase (PARP). *Arkivoc*, 121-131 (2003).
72. Deres, L. et al. PARP-inhibitor treatment prevents hypertension induced cardiac remodeling by favorable modulation of heat shock proteins, Akt-1/GSK-3beta and several PKC isoforms. *PLoS One* **9**, e102148 (2014).
73. Bartha, E. et al. Effect of L-2286, a poly(ADP-ribose)polymerase inhibitor and enalapril on myocardial remodeling and heart failure. *J Cardiovasc Pharmacol* **52**, 253-61 (2008).
74. Palfi, A. et al. PARP inhibition prevents postinfarction myocardial remodeling and heart failure via the protein kinase C/glycogen synthase kinase-3beta pathway. *J Mol Cell Cardiol* **41**, 149-59 (2006).
75. Kubota, Y. et al. Evaluation of blood pressure measured by tail-cuff methods (without heating) in spontaneously hypertensive rats. *Biol Pharm Bull* **29**, 1756-8 (2006).
76. Ruifrok, A.C. & Johnston, D.A. Quantification of histochemical staining by color deconvolution. *Anal Quant Cytol Histol* **23**, 291-9 (2001).

77. Hocsak, E. et al. PARP inhibition protects mitochondria and reduces ROS production via PARP-1-ATF4-MKP-1-MAPK retrograde pathway. *Free Radic Biol Med* **108**, 770-784 (2017).
78. Guillamon-Vivancos, T., Gomez-Pinedo, U. & Matias-Guiu, J. Astrocytes in neurodegenerative diseases (I): function and molecular description. *Neurologia* **30**, 119-29 (2015).
79. English, F.A. et al. Administration of the PARP inhibitor Pj34 ameliorates the impaired vascular function associated with eNOS(-/-) mice. *Reprod Sci* **19**, 806-13 (2012).
80. Zerfaoui, M. et al. Poly(ADP-ribose) polymerase-1 is a determining factor in Crm1-mediated nuclear export and retention of p65 NF-kappa B upon TLR4 stimulation. *J Immunol* **185**, 1894-902 (2010).
81. Radovits, T. et al. Poly(ADP-ribose) polymerase inhibition improves endothelial dysfunction induced by reactive oxidant hydrogen peroxide in vitro. *Eur J Pharmacol* **564**, 158-66 (2007).
82. Radovits, T. et al. Single dose treatment with PARP-inhibitor INO-1001 improves aging-associated cardiac and vascular dysfunction. *Exp Gerontol* **42**, 676-85 (2007).
83. Li, C.Y., Yang, L.C., Guo, K., Wang, Y.P. & Li, Y.G. Mitogen-activated protein kinase phosphatase-1: a critical phosphatase manipulating mitogen-activated protein kinase signaling in cardiovascular disease (review). *Int J Mol Med* **35**, 1095-102 (2015).
84. Ushio-Fukai, M., Alexander, R.W., Akers, M. & Griendling, K.K. p38 Mitogen-activated protein kinase is a critical component of the redox-sensitive signaling pathways activated by angiotensin II. Role in vascular smooth muscle cell hypertrophy. *J Biol Chem* **273**, 15022-9 (1998).
85. Halmosi, R. et al. Effect of poly(ADP-ribose) polymerase inhibitors on the ischemia-reperfusion-induced oxidative cell damage and mitochondrial metabolism in Langendorff heart perfusion system. *Mol Pharmacol* **59**, 1497-505 (2001).
86. Pacher, P. et al. The role of poly(ADP-ribose) polymerase activation in the development of myocardial and endothelial dysfunction in diabetes. *Diabetes* **51**, 514-21 (2002).
87. Modis, K. et al. Cellular bioenergetics is regulated by PARP1 under resting conditions and during oxidative stress. *Biochem Pharmacol* **83**, 633-43 (2012).
88. Douglas, D.L. & Baines, C.P. PARP1-mediated necrosis is dependent on parallel JNK and Ca(2)(+)/calpain pathways. *J Cell Sci* **127**, 4134-45 (2014).
89. Tapodi, A. et al. Pivotal role of Akt activation in mitochondrial protection and cell survival by poly(ADP-ribose)polymerase-1 inhibition in oxidative stress. *J Biol Chem* **280**, 35767-75 (2005).
90. Yu, S.W. et al. Outer mitochondrial membrane localization of apoptosis-inducing factor: mechanistic implications for release. *ASN Neuro* **1** (2009).
91. Brunyanszki, A., Szczesny, B., Virag, L. & Szabo, C. Mitochondrial poly(ADP-ribose) polymerase: The Wizard of Oz at work. *Free Radic Biol Med* **100**, 257-270 (2016).
92. Masmoudi, A., Islam, F. & Mandel, P. ADP-ribosylation of highly purified rat brain mitochondria. *J Neurochem* **51**, 188-93 (1988).
93. Rossi, M.N. et al. Mitochondrial localization of PARP-1 requires interaction with mitofilin and is involved in the maintenance of mitochondrial DNA integrity. *J Biol Chem* **284**, 31616-24 (2009).

94. MacVicar, T. & Langer, T. OPA1 processing in cell death and disease - the long and short of it. *J Cell Sci* **129**, 2297-306 (2016).
95. Twig, G. et al. Fission and selective fusion govern mitochondrial segregation and elimination by autophagy. *EMBO J* **27**, 433-46 (2008).
96. Crabtree, G.R. Generic signals and specific outcomes: signaling through Ca2+, calcineurin, and NF-AT. *Cell* **96**, 611-4 (1999).
97. Riehle, C. & Abel, E.D. PGC-1 proteins and heart failure. *Trends Cardiovasc Med* **22**, 98-105 (2012).
98. Zhang, T. et al. Enzymes in the NAD+ salvage pathway regulate SIRT1 activity at target gene promoters. *J Biol Chem* **284**, 20408-17 (2009).
99. Zhang, T. et al. Regulation of poly(ADP-ribose) polymerase-1-dependent gene expression through promoter-directed recruitment of a nuclear NAD+ synthase. *J Biol Chem* **287**, 12405-16 (2012).
100. Pirinen, E. et al. Pharmacological Inhibition of poly(ADP-ribose) polymerases improves fitness and mitochondrial function in skeletal muscle. *Cell Metab* **19**, 1034-41 (2014).
101. Canto, C. & Auwerx, J. PGC-1alpha, SIRT1 and AMPK, an energy sensing network that controls energy expenditure. *Curr Opin Lipidol* **20**, 98-105 (2009).

9. Acknowledgement

I wish to express my gratefulness to my Program Leader, Professor Kálmán Tóth, and to my Project Leader, Dr. Halmosi Róbert for guiding my studies throughout the field of cardiovascular sciences and providing the possibility of the current work. I'm genuinely appreciative to Professor Balázs Sümegi for mentoring my studies and work in the recent years and for widening my view on systemic biology.

I'm thankful to all my present and former colleagues, especially for Dr. Klára Magyar and for Dr. László Deres, for their contributions and helping hands in the present research. Notably, my sincerest appreciation to Professor László Seress, for his immense field support in respect to hippocampal observations. Addtionally, I wish to acknowledge Mrs. Tímea Dózsa and Mr. József Nyiradi, for extending their expertise in support of this body of research.

I want to offer my thanks to Dr. Ildikó Bock-Marquette and Mr. Jon E. Marquette for their encouraging words and mentality throughout these times.

I express my warmest appreciation to my family and close friends for their immense patience and support during the preparation of this work.